ELSEVIER

Contents lists available at ScienceDirect

Marine Micropaleontology

journal homepage: www.elsevier.com/locate/marmicro





Diatoms of the intertidal environments of Willapa Bay, Washington, USA as a sea-level indicator

Isabel Hong ^{a,*,1}, Benjamin P. Horton ^b, Andrea D. Hawkes ^c, Robert J. O'Donnell III ^c, Jason S. Padgett ^d, Tina Dura ^e, Simon E. Engelhart ^f

- ^a Department of Geological Sciences, Central Washington University, Ellensburg, WA 98926, USA
- ^b Earth Observatory of Singapore and the Asian School of the Environment, Nanyang Technological University, Singapore
- ^c Department of Earth and Ocean Sciences, Center for Marine Science, University of North Carolina Wilmington, Wilmington, NC 28403, USA
- ^d Department of Geosciences, University of Rhode Island, Kingston, RI, USA
- e Department of Geosciences, Virginia Polytechnic Institute and State University, Blacksburg, VA 24061, USA
- f Department of Geography, Durham University, Durham DH1 3LE, UK

ARTICLE INFO

Keywords: Tidal wetland Relative sea level Cascadia Earthquakes Subduction zone

ABSTRACT

An understanding of the modern relationship between diatom species and elevation is a prerequisite for using fossil diatoms to reconstruct relative sea level (RSL). We described modern diatom distributions from seven transects covering unvegetated subtidal environments to forested uplands from four tidal wetland sites (Smith Creek, Bone River, Niawiakum River, and Naselle River) of Willapa Bay, Washington, USA. We compared our diatom dataset (320 species from 104 samples) to a series of environmental variables (elevation, grain-size, total organic carbon (TOC_{SOM}), and porewater salinity) using hierarchical clustering and ordination. While no single variable consistently explains variations in diatom assemblages at every site, elevation, salinity, and substrate (mud fraction and TOC_{SOM}) are variables affecting diatom distribution along our transects. Elevation was the major environmental control of diatom variability (explained 27-39% variance) at four transects (Bone River Transect 1, Niawiakum River Transect 2, Naselle River Transect 1 and 2). Salinity and substrate were the major environmental controls (explained 12-32% variance) of diatom variability at three transects (Niawiakum River Transect 1: salinity; Smith Creek Transect and Bone River Transect 2: TOC_{SOM}). Analyses of a combined regional dataset of all transects suggest that elevation is the driver of regional diatom variability in Willapa Bay, with salinity and substrate co-varying along an elevation gradient. We identify species with narrow elevation tolerances that can serve as indicator species of specific environments. Despite the site-specific variability of our modern diatom distribution, the regional dataset provides an important dataset that can be used to reconstruct RSL in Willapa Bay.

1. Introduction

Diatoms are photosynthetic algae that are widely applied in paleo-environmental reconstructions (e.g., Birks et al., 1990; Fritz et al., 1991; Battarbee et al., 2002) because they are abundant in marine, brackish, and freshwater environments (e.g., Conger, 1951; Admiraal, 1984; Palmer and Abbott, 1986). Diatom species preferences for distinct environments has led to multiple paleoenvironmental classification systems based on salinity, substrate, and elevation with respect to tide levels (e.g., Hustedt, 1937, 1939, 1953, 1957; Denys, 1991; Vos and de Wolf, 1993; Zong and Horton, 1998). Furthermore, the short life cycle of

diatoms allows for the rapid colonization of new species in response to sudden environmental change (Oemke and Burton, 1986; Denys, 1991; Vos and de Wolf, 1993; Hirst et al., 2004; Horton et al., 2017).

Diatoms have been applied to estimate relative sea-level (RSL) change during prehistoric megathrust earthquakes at the Cascadia subduction zone (e.g., Darienzo and Peterson, 1990; Shennan et al., 1994; Nelson and Kashima, 1993; Hemphill-Haley, 1995a, 1995b; Atwater and Hemphill-Haley, 1997; Sawai et al., 2016). The elevation with respect to tide levels of modern diatom assemblages serve as an analog from which fossil diatom assemblages are used to reconstruct RSL (e.g., Haggart, 1986; Shennan et al., 1996; Zong and Horton, 1999;

https://doi.org/10.1016/j.marmicro.2021.102033

Received 26 March 2021; Received in revised form 23 July 2021; Accepted 27 July 2021 Available online 30 July 2021

^{*} Corresponding author at: Department of Geological Sciences, Central Washington University, 400 East University Way, Ellensburg, WA 98926, USA. *E-mail address:* isabel.hong@cwu.edu (I. Hong).

Department of Earth Sciences, Simon Fraser University, BC, V5A 1S6, Canada.

Sawai et al., 2004a; Watcham et al., 2013; Shennan and Hamilton, 2006). Across the intertidal zone, changes in diatom assemblages display a vertical zonation corresponding to changes in environmental variables (e.g., salinity and substrate) that are related to tidal exposure (e.g., Vos and de Wolf, 1993; Hemphill-Haley, 1995b; Sherrod, 1999; Horton et al., 2006, 2007; Sawai et al., 2016). However, diatom-based estimates of RSL change have been hampered by the site-specific diversity of diatom assemblages that can result in matching analog issues with fossil diatoms in sediment cores (e.g., Nelson and Kashima, 1993; Nelson et al., 2008; Garrett et al., 2013; Nelson et al., 2020; Brader et al., 2020). Therefore, it is important to compile modern datasets from a wide range of elevations and a diversity of environments (i.e., marine to freshwater environments; varied site geomorphologies and settings) to better improve our understanding of species distributions across the intertidal zone (Watcham et al., 2013; Sawai et al., 2016).

Here, we describe and quantify variability in diatom distributions from tidal wetlands of Willapa Bay, Washington that has produced a 3500-year record of multiple Cascadia megathrust earthquakes preserved in intertidal stratigraphic sequences as mud-over-peat contacts (Atwater, 1987; Hemphill-Haley, 1995a, 1995b; Atwater and Hemphill-Haley, 1997). We analyzed the diatom assemblages in 104 samples and the environmental variables (elevation, grain-size, total organic carbon (TOC_{SOM}), and porewater salinity) that control their distribution from seven transects in eastern Willapa Bay (Fig. 1): Smith Creek (1 transect); Bone River (2 transects); Niawiakum River (2 transects); and Naselle

River (2 transects). Hierarchical clustering and ordination show site variability in diatom zonation due to differing responses to environmental variables. We conclude with considerations for diatom-based RSL reconstructions.

2. Study area

Willapa Bay (Fig. 1) is a drowned-river valley estuary formed during flooding of the valley because of gradual RSL rise during the early to mid-Holocene (e.g., Emmett et al., 2000; Engelhart et al., 2015; Dura et al., 2016a). Sediment supplied by the Columbia River produced a 26-km long barrier spit ~5000 years ago (Smith et al., 1999) that protects Willapa Bay from the Pacific Ocean (Emmett et al., 2000), resulting in low-energy wetland environments conducive for the reconstruction of former sea levels. Furthermore, Willapa Bay provides a relatively unmodified natural environment in which to study the modern distribution of diatoms because human and industrial disturbance has been minimal, as much of its wetland is nationally or state-protected (Emmett et al., 2000).

The climate at Willapa Bay is temperate. We sampled in May 2015 and August 2019 during which the average daily temperatures (May 2015: High 16.8 °C Low 8.2 °C; August 2019: High 23.2 °C Low 10.6 °C) were similar to historical average temperatures in May 2015 (High 17.1 °C, Low 5.4 °C) and August 2019 (High 22.8 °C, Low 9.4 °C; NCDC, 2019). Mean daily precipitation (May 2015: 298 mm; August 2019: 30.5

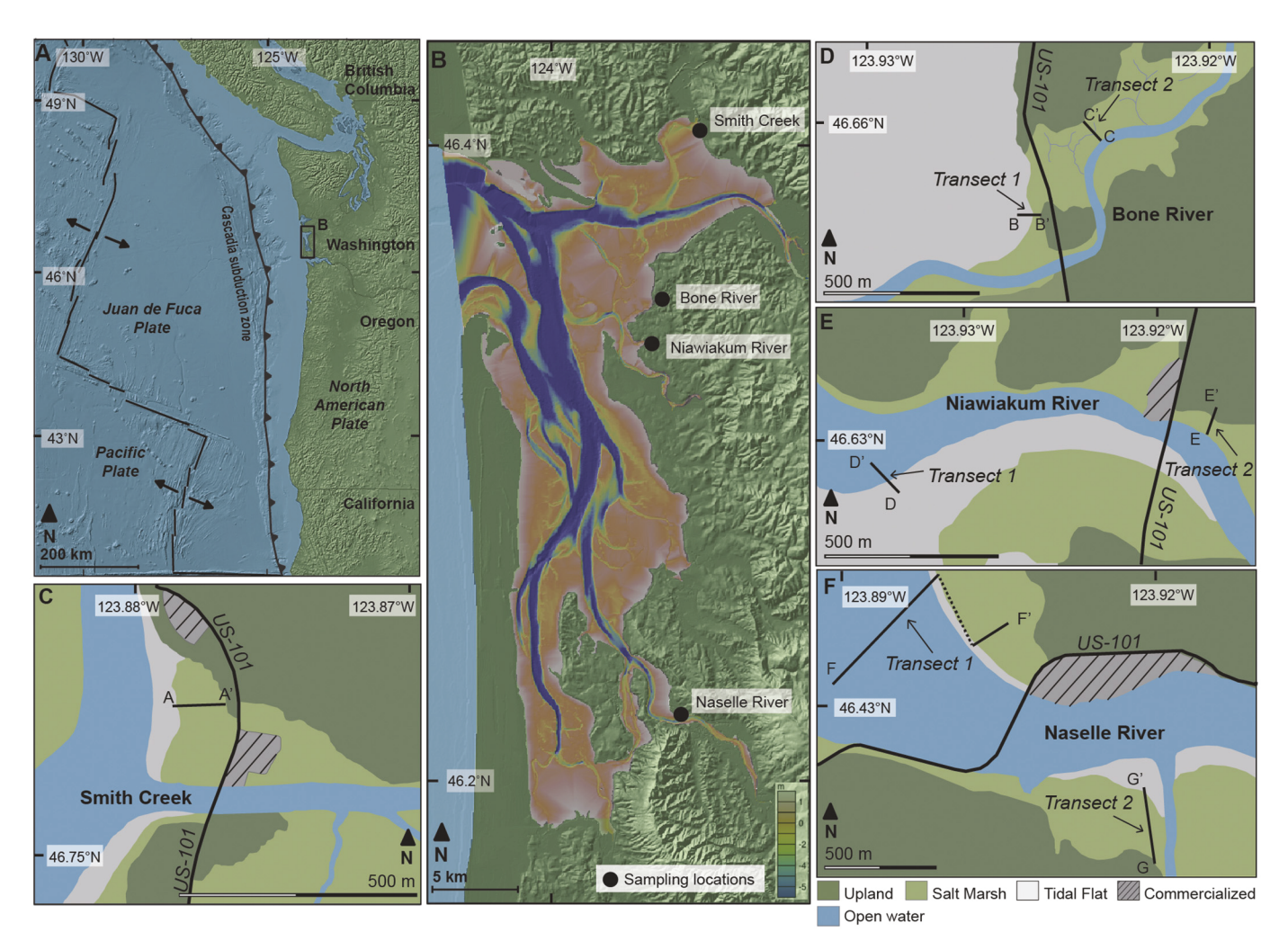


Fig. 1. (A) Map of the Cascadia subduction zone and its major features. (B) Bathymetry of Willapa Bay, WA (50 m resolution; NOAA, 2016) with sampling sites marked by circles. (C) Smith Creek with sampled transect marked with a solid black line. (D) Bone River with sampled transects marked with solid black lines. (E) Niawiakum River with sampled transects marked with solid black lines. (F) Naselle River with sampled transects marked with solid black lines.

mm) was also similar to the historical mean in May 2015 (323 mm) and August 2019 (35.3 mm; NCDC, 2019).

Tides at Willapa Bay are mixed semidiurnal (NOAA, 2019). At Smith Creek, Bone River, and Niawiakum River, the Great Diurnal range (difference of mean higher high water and mean lower low water) is 2.8 m (NOAA, 2019). At the Naselle River in southern Willapa Bay, the Great Diurnal range is 3.3 m (NOAA, 2019). The bathymetry of Willapa Bay shows an extensive tidal flat incised with three main channels that range in depth from 9 to 24 m (Fig. 1b; Olabarrieta et al., 2011).

The vascular plant communities of Willapa Bay's wetlands can be grouped into four zones: tidal flat, low marsh, high marsh, and forested upland (Hemphill-Haley, 1995a, 1995b; Atwater and Hemphill-Haley, 1997; Cooke, 1997). The subtidal environment (below mean lower low water) is largely defined by deep tidal channels that lack vascular plant cover (e.g., Gingras et al., 1999; Banas and Hickey, 2005). Tidal flats (below mean low water) contain only sparse amounts of Zostera sp. The low marsh (commonly below mean high water) is characterized by tidal flat colonizers Glaux maritima, Jaumea carnosa, Salicornia virginica, Spartina alterniflora (a non-native introduced species), and Triglochin maritima. The high marsh is commonly characterized by Carex lyngbyei, Deschampsia caespitosa, Distichlis spicata, Juncus balticus, and Potentilla pacifica. Forested swamps and uplands include trees, commonly Picea sitchensis and Pyrus fusca.

We selected four tidal wetland sites spread across the length Willapa Bay with the aim of capturing the wide ecological tolerance of modern diatom assemblages (Fig. 1b). The northernmost site, Smith Creek (Transect 1 spans the tidal flat to high marsh), is the fourth largest river (23-km-long) in Willapa Bay, draining to join the two largest rivers (North River and Willapa River) in forming the eastward arm of the bay (Fig. 1b). Moving south, Bone River (Transect 1 spans the tidal flat to upland and Transect 2 spans the high marsh) and Niawiakum River (Transect 1 spans the subtidal to tidal flat and Transect 2 spans the tidal flat to high marsh) are two of the smallest rivers in Willapa Bay (9- and 11-km-long, respectively) and are designated Natural Area Preserves that contain broad, undisturbed salt marshes (Emmett et al., 2000). The Naselle River (Transect 1 spans the tidal flat to upland and Transect 2 spans the low marsh to high marsh) marks our southernmost location and is the third largest river in Willapa Bay, producing up to 18% of freshwater input into the bay (Banas and Hickey, 2005).

3. Methods

3.1. Field sampling and elevation measurement

We sampled 104 stations along seven elevation transects (Smith Creek Transect, Bone River Transect 1 and 2, Niawiakum River Transect 1 and 2, Naselle River Transect 1 and 2) from the subtidal to forested uplands of eastern Willapa Bay (Fig. 1). Two transects were collected at Bone River, Niawiakum River, and Naselle River to incorporate a wider range of environments that could not be captured in a single transect. Samples were collected at approximately 10- to 20- cm vertical increments except where adjacent stations crossed a steep slope resulting in a sudden transition in elevation. Subtidal samples were collected using an Ekman grab sampler deployed from a canoe. Intertidal and forested upland samples were collected using a knife. The upper 2 mm of surface sediment was subsampled for diatom, grain-size, TOC_{SOM}, and porewater salinity analyses. We estimated the percent cover of the dominant vascular plant species at our sampling stations using Cooke (1997) as a reference. Sediment samples were refrigerated after collection and prior to laboratory analyses.

We measured the elevation of intertidal and upland sampling stations using a Leica GS-15 Real Time Kinematic-Global Positioning System (RTK-GPS) and total station. Error estimates on these measurements are <4 cm. To establish elevations of subtidal sampling stations with respect to the tidal datum, we used a handheld water sounder and depth meter and conducted regular measurements (every 6 min) of tide levels

using the RTK-GPS. Elevations of all stations were referenced to the North American Vertical Datum (NAVD88) and tied to mean tide level (MTL) using the VDatum transformation software (NOAA, Accessed 2019). We converted our measured elevations to a standardized water level index (SWLI) to allow comparison among sites with differing tidal ranges where MTL is 100 SWLI and MHHW is 200 SWLI (Horton et al., 1999).

3.2. Diatom and environmental analyses

Diatom analysis followed Palmer and Abbott (1986). In the laboratory, 1 cm³ of sediment was placed in a 25-mL plastic Falcon tube with 30% concentration H₂O₂ until no organic material remained. We dripped (5-40 µL concentration), dried, and mounted the diatoms onto a glass slide using Naphrax. For each sample, 400 valves were counted using light microscopy under oil immersion at 1000× magnification with abundance calculated as a percentage of total diatom valves counted. We denote rare species as having a maximum abundance of ≤5% in a single sample and abundant species as having a maximum abundance of >10% in a single sample. Diatoms were identified to species level using Krammer and Lange-Bertalot (1986, 1988, 1991a, 1991b), and Witkowski (2000) and classified by salinity based on local (Hemphill-Haley, 1995a, 1995b, 1996; Sawai et al., 2016) and global observations (Krammer and Lange-Bertalot, 1986, 1988, 1991a, 1991b; Denys, 1991; Witkowski, 2000) into marine, brackish and freshwater (includes fresh-brackish and freshwater) species.

To characterize the relationship between diatom assemblages and environmental variables, we analyzed three variables from surface sediment at each sampling station: grain-size, TOC_{SOM}, and porewater salinity concentrations. We prepared each sample for grain-size analysis by placing sediment from each station in a 25 mL plastic Falcon tube and removing organic matter using 30% concentration H₂O₂ (Donato et al., 2009). We measured grain-size using a Malvern Mastersizer 3000 laser particle-size analyzer (Sperazza et al., 2004) and use mud fraction to characterize grain-size (e.g., Sawai et al., 2016). Bulk sedimentary organic matter (SOM) for TOC_{SOM} composition was analyzed at the University of North Carolina-Wilmington (O'Donnell III, 2017). The samples were dried at 50 °C for 24 h prior to being ground with a mortar and pestle. Bulk values are reported relative to the Vienna Pee Dee Belemnite scale using L-glutamic acid (USGS40, USGS41, and USGS41a). We calculated the percent TOC_{SOM} by using the known weight of each sample, quantity of C in the L-glutamic acid standards, and the relative production of CO₂ after combustion. We centrifuged the samples to extract porewater salinity prior to measurement with a calibrated refractometer (Sherrod, 1999; Sawai et al., 2016). When no porewater was present, 5 mL of deionized water was added to samples before centrifuging and measurement (e.g., Sawai et al., 2016; Desianti et al., 2019).

3.3. Statistical analysis

We employed hierarchical clustering to identify groups of diatom assemblages within each transect and from all transects combined (e.g., van Togeren, 1987; Theriot, 1992; Zong and Horton, 1998). We classified the modern samples using Ward's minimum unconstrained cluster analysis based on unweighted Euclidean distance using PAST software (Hammer et al., 2001). The number of clusters was determined using the broken-stick method (MacArthur, 1957) using the software R version 4.0.3 (R Core Development Team, 2020) and the cluster package (Maechler et al., 2019).

We analyzed the relationship between modern diatom assemblages and environmental variables of samples along each transect as well as among all transects combined using the ordination method of principal component analysis (PCA; ter Braak, 1986). PCA relates community composition to environmental variables by reducing the dimensions to principal components (axes) that represent the maximum variance

between species assemblages and environmental variables (e.g., Abdi and Williams, 2010). The gradient lengths of the environmental vectors on the PCA sample-environment biplot approximate their relative importance in explaining the variance in the diatom data, whereas their orientation demonstrates the approximate correlation to the ordination axes as well as to other environmental variables (ter Braak, 1986). Redundancy analysis (RDA) identified the total variance in diatom assemblages that can be explained by the environmental variables. RDA was chosen because the gradient length of individual transects ranged from 1.5 to 2.9 SD with only two transects (Niawiakum River Transect 2 and Naselle River Transect 2) exceeding a gradient length of 2 SD (ter Braak, 1986; Birks, 1995). We determined the contribution of each variable to diatom assemblage variance using constrained analysis and interactive-forward-selection, using a *p* value < 0.01 as the threshold for a variable to be considered a major control. To test the influence of site variability on diatom zonation, we include each site as a factor (categorical) variable in our RDA of our regional dataset following the methods of Lepš and Šmilauer (2003) whereby each sample is given a numeric value based on its presence (1) or absence (0) at a site. Determination of gradient length as well as PCA and RDA analyses were performed using the software CANOCO version 4.5 (ter Braak and Smilauer, 1998, 2002). Descriptive statistics of the elevation

distribution of the regional dataset was performed using the software R (R base; R Core Development Team, 2020).

We used weighted averaging (e.g., ter Braak, 1985; ter Braak and Barendregt, 1986; Birks, 1995) to quantify the abundance and distribution of taxa across elevation as a function of tidal exposure (e.g., Zong and Horton, 1999) because the calculated gradient length (2.9 SD) of the combined regional dataset indicates a unimodal response (ter Braak, 1986; Birks, 1995; ter Braak and Smilauer, 2002). For weighted averaging, rare species were excluded from analysis. We calculated the optima (weighted averages) and tolerance (weighted average standard deviations) range of diatom species to elevation (SWLI) from the combined regional dataset using the software C2 version 1.7.7 (Juggins, 2012)

For all statistical analyses, we used the relative percent (calculated as a percentage of total diatom valves counted) of all species counted in each sample.

4. Results

4.1. Smith Creek

Smith Creek Transect is comprised of 10 sampling stations ranging in

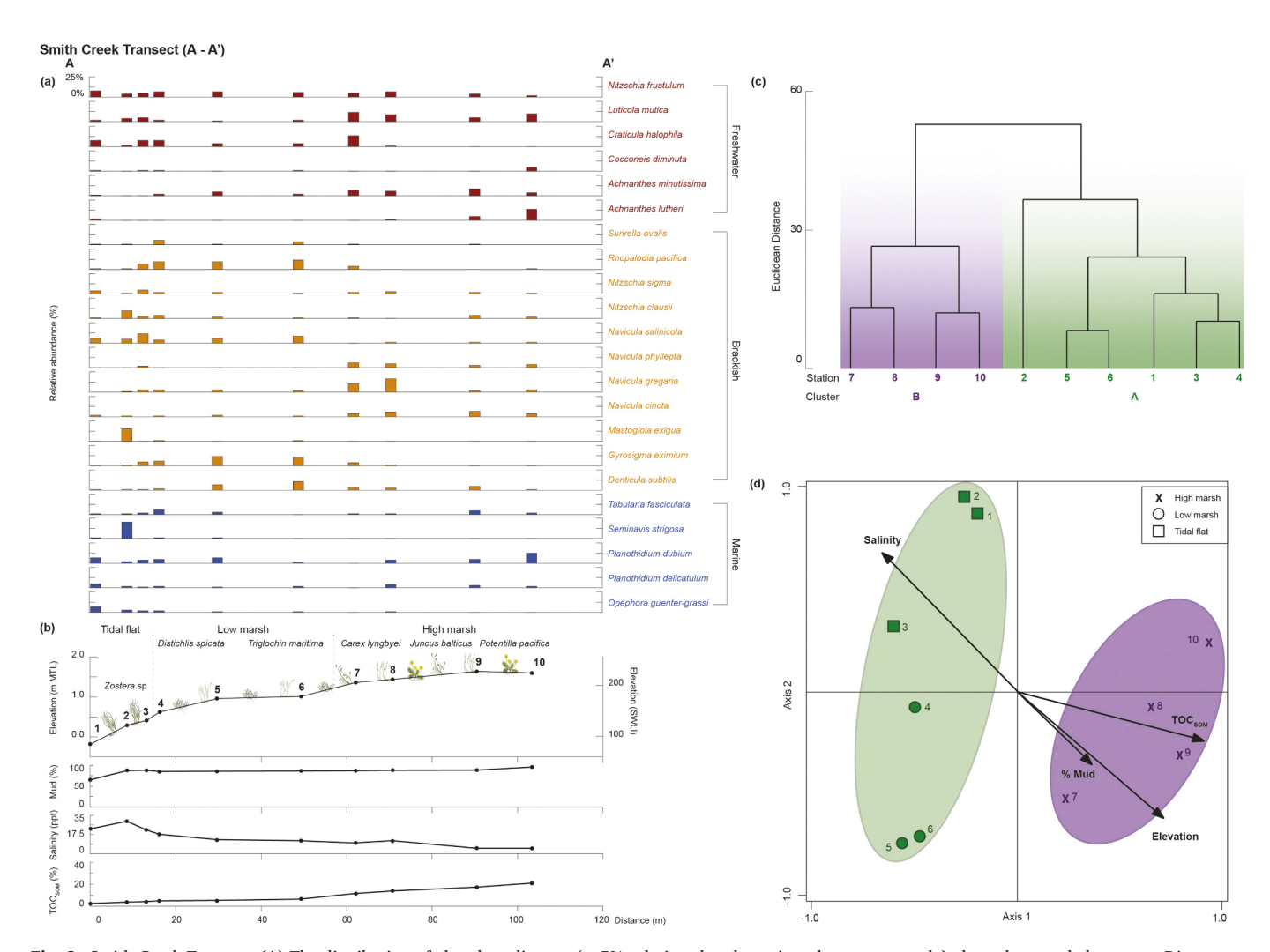


Fig. 2. Smith Creek Transect. (A) The distribution of abundant diatoms (\geq 5% relative abundance in at least one sample) along the sampled transect. Diatoms are separated based on their salinity preferences (blue: marine; yellow: brackish; red: freshwater). (B) Sampled transect showing the location of the sampling stations and major vascular vegetation separated by zones relative to distance and elevation. The mud fraction, salinity (ppt), and TOC_{SOM} of each sampling station is plotted relative to distance. (C) Results of hierarchical cluster analysis with (D) PCA sample-environment biplot results shown below. Station symbols indicate their sampling location (square: tidal flat; circle: low marsh; cross: high marsh). (For interpretation of the references to colour in this figure legend, the reader is referred to the web version of this article.)

elevation from -0.18 to 1.64 m above MTL (86 to 226 SWLI) that spans the tidal flat to high marsh vascular vegetation environments (Fig. 2). Vegetation across the transect consists of sparse *Zostera* sp. on the tidal flat (Stations 1–3), *D. spicata* and *T. maritima* on the low marsh (Stations 4–6), and dominantly *C. lyngbyei, J. balticus*, and *P. pacifica* on the high marsh (Stations 7–10). Grain-size analysis shows the relative percent of mud remains relatively constant (89 to 100%) across the transect except for Station 1 (68%). Salinity ranges from 5 to 30 ppt and generally decreases with increasing elevation across the transect. TOC_{SOM} increases from 2 to 20% with elevation.

We identified 152 species from 49 genera along the Smith Creek Transect. Marine species ($Seminavis\ strigosa: \le 21\%$) and brackish species ($Mastogloia\ exigua: \le 16\%$, $Navicula\ salinicola: \le 12\%$, and $Nitzschia\ clausii: \le 11\%$) are abundant in the tidal flat. Brackish species ($Denticula\ subtilis: \le 11\%$), $Gyrosigma\ eximium: \le 12\%$, and $Rhopalodia\ pacifica: \le 12\%$) are abundant throughout the low marsh. Freshwater species ($Achnanthes\ lutheri: \le 14\%$, $Craticula\ halophila: \le 14\%$, and Luticola mutica: $\le 12\%$) are abundant in high marsh samples.

Hierarchical clustering identified two diatom groups along the Smith Creek Transect (Fig. 2). Cluster A consists of tidal flat and low marsh Stations $1{\text -}6$ with an elevation range of -0.18 to 1.01 m above MTL (86 to 178 SWLI). We observe marine and brackish species in Cluster A. Cluster B consists of high marsh samples from Stations $7{\text -}10$ with an elevation range of 1.36 to 1.60 m above MTL (206 to 227 SWLI). In contrast to Cluster A, we observe freshwater and brackish species in Cluster B.

PCA produced Axis 1 with an eigenvalue of 0.35 and Axis 2 with an eigenvalue of 0.22 that explains 57% of the total variance in the diatom assemblages (Table 1) with 70% explained by the environmental variables (Table 2). Intra-set correlations of environmental variables with axes 1 and 2 show that TOC_{SOM} is correlated with Axis 1 and that salinity, elevation, and mud fraction are correlated with both axes 1 and 2 (Fig. 2). Constrained and interactive-forward-selection analyses identify TOC_{SOM} (explains 32% variance) and elevation (explains 19% variance) as major explanatory variables with salinity (explains 11% variance) and mud fraction (explains 9% variance) as minor explanatory variables (Table 2).

Table 1Summary PCA results with eigenvalues and explained cumulative variation of local and regional dataset.

Transect	Statistic	Axis	Axis	Axis	Axis
		1	2	3	4
	Eigenvalue	0.35	0.22	0.10	0.09
	Explained cumulative				
Smith Creek	variation	35%	57%	67%	76%
	Eigenvalue	0.38	0.18	0.09	0.06
	Explained cumulative				
Bone River 1	variation	38%	56%	65%	71%
	Eigenvalue	0.22	0.20	0.12	0.08
	Explained cumulative				
Bone River 2	variation	22%	41%	54%	62%
	Eigenvalue	0.37	0.16	0.10	0.08
Niawiakum	Explained cumulative				
River 1	variation	37%	53%	63%	72%
	Eigenvalue	0.34	0.15	0.10	0.06
Niawiakum	Explained cumulative				
River 2	variation	34%	49%	59%	65%
	Eigenvalue	0.36	0.15	0.09	0.05
	Explained cumulative				
Naselle River 1	variation	36%	51%	60%	64%
	Eigenvalue	0.42	0.20	0.13	0.11
	Explained cumulative				
Naselle River 2	variation	42%	62%	76%	86%
	Eigenvalue	0.21	0.09	0.08	0.06
	Explained cumulative				
Regional Dataset	variation	21%	31%	39%	45%

Table 2Summary RDA results of local and regional dataset showing total variance in diatom assemblages explained by the environmental variables.

Smith Creek Transect		Bone River Transect 1		
Variable	Contribution (%)	Variable	Contribution (%)	
TOC	32	Elevation	35	
Elevation	19	TOC	14	
Salinity	11	% Mud	7	
% Mud	9	Salinity	6	
Total	70	Total	63	

Bone River Transect 2		Niawiakum River Transect 1		
Variable	Contribution (%)	Variable Contribution (
TOC	20	Salinity	31	
Salinity	10	% Mud	12	
Elevation	8	TOC	11	
% Mud	6	Elevation	7	
Total	44	Total	61	

Niawiakum River Transect 2		Naselle River Transect 1		
Variable	Contribution (%)	Variable	Contribution (%)	
Elevation	28	Elevation	27	
Salinity	14	Salinity	8	
TOC	6	TOC	5	
% Mud	4	% Mud	4	
Total	52	Total	44	

Naselle River Transect 2		Regional Dataset		
Variable	Contribution (%)	Variable	Contribution (%)	
Elevation	39	% Mud	12	
TOC	21	TOC	11	
% Mud	10	Salinity	10	
Salinity	9	Elevation	9	
Total	79	Site	5	
		Total	47	

4.2. Bone River

4.2.1. Transect 1

Bone River Transect 1 is comprised of 16 sampling stations ranging in elevation from 0.50 to 1.99 m above MTL (139 to 256 SWLI) that spans the tidal flat to upland (Fig. 3). Vegetation across the transect consists of sparse *Zostera* sp. on the tidal flat (Stations 1–6), *S. virginica* and *T. maritima* on the low marsh (Stations 7–11), and *D. spicata* and *P. pacifica* in the high marsh (Stations 12–15). Sitka spruce (*P. sitchensis*) and Western crabapple (*P. fusca*) are the dominant tree species on the upland (Station 16). Grain-size analysis shows a shift from mostly sand on the tidal flat (60 to 77% sand) to mud dominating the salt marsh and upland; the maximum mud content was at Station 11 (98% mud). Salinity ranges from 4 to 35 ppt and decreases with increasing elevation with a sharp change from Station 9 to 10 (33 to 16 ppt) at the transition from low to high marsh. TOC_{SOM} increases with elevation, with a notable increase of >20% organic carbon from Station 13 to 14 where there is a transition from high marsh to upland.

We identified 173 species from 53 genera along the transect. *Planothidium delicatulum* was dominant (\geq 15% abundance) in the tidal flat. Marine species (Cocconeis scutellum var parva: \leq 18% *Opephora minuta*: \leq 19%, and *Pravifusus hyalinus*: \leq 10%) are abundant in tidal flat samples. Brackish species (*Navicula gregaria*: \leq 6%, *Navicula perminuta*: \leq 6%, and *R. pacifica*: \leq 7%) only exceed rare abundance in low marsh samples. The freshwater species *Melosira varians, Nitzschia frustulum*, and *Pinnularia lagerstedtii* are only present at \leq 10% abundance in the high marsh and upland. *Cocconeis scutellum*, an epiphytic (attachment to aquatic plants) species commonly found across the intertidal due to its allochthonous (transported) component, was dominant (19–41%

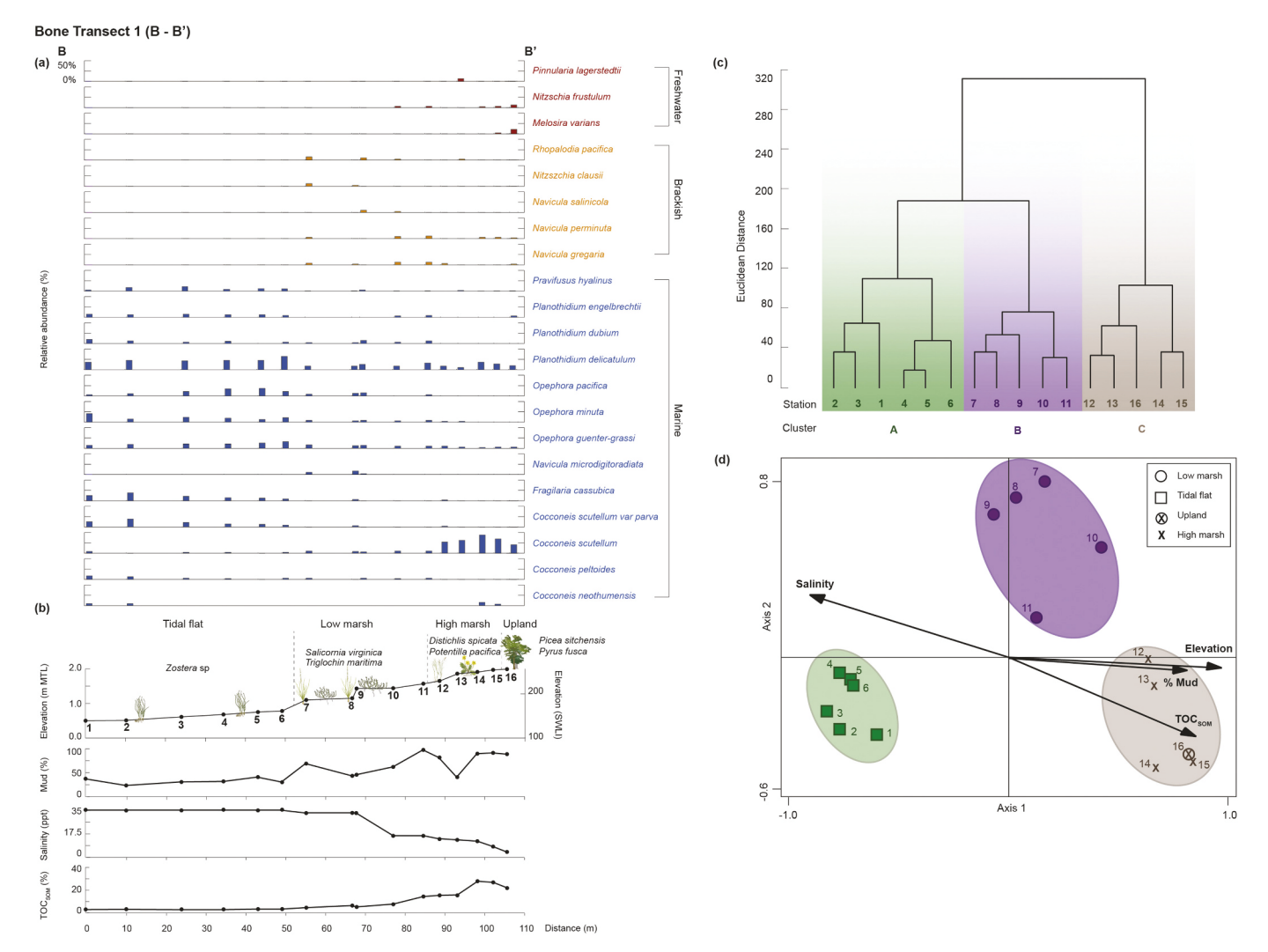


Fig. 3. Bone River Transect 1. (A) The distribution of abundant diatoms ($\geq 5\%$ relative abundance in at least one sample) along the sampled transect. Diatoms are separated based on their salinity preferences (blue: marine; yellow: brackish; red: freshwater). (B) Sampled transect showing the location of the sampling stations and major vascular vegetation separated by zones relative to distance and elevation. The mud fraction, salinity (ppt), and TOC_{SOM} of each sampling station is plotted relative to distance. (C) Results of hierarchical cluster analysis with (D) PCA sample-environment biplot results shown below. Station symbols indicate their sampling location (square: tidal flat; circle: low marsh; cross: high marsh; crossed circle: upland). (For interpretation of the references to colour in this figure legend, the reader is referred to the web version of this article.) (For interpretation of the references to colour in this figure legend, the reader is referred to the web version of this article.)

abundance) at the higher elevation stations.

Hierarchical clustering identified three diatom groups along Bone River Transect 1 (Fig. 3). Cluster A consists of tidal flat samples from Stations 1–6 with an elevation range of 0.50 to 0.78 m above MTL (139 to 162 SWLI). In contrast to the other two groups, brackish and freshwater species are very rare (< 2% abundance) in Cluster A. Cluster B consists of low marsh samples and brackish species from Stations 7–11 with an elevation range of 1.10 to 1.57 m above MTL (186 to 223 SWLI). Cluster C consists of high marsh and upland samples from Stations 12–16 with an elevation range of 1.65 to 1.99 m above MTL (230 to 256 SWLI). Freshwater species only exceed rare abundance in Cluster C. High abundances of *C. scutellum* also occur in Cluster C.

PCA produced an Axis 1 with an eigenvalue of 0.38 and an Axis 2 with an eigenvalue of 0.18 that explains 56% of the total variance in the diatom assemblages (Table 1) with 62% explained by the environmental variables (Table 2). Intra-set correlations of variables with axes 1 and 2 show that elevation and mud fraction are correlated with Axis 1 and that TOC_{SOM} and salinity are correlated with both axes 1 and 2 (Fig. 3). Constrained and interactive-forward-selection analyses identify elevation (explains 35% variance) and TOC_{SOM} (explains 14% variance) as

major explanatory variables with mud fraction (explains 7% variance) and salinity (explains 6% variance) as minor explanatory variables (Table 2).

4.2.2. Transect 2

Bone River Transect 2 is comprised of 13 sampling stations in the high marsh with a relatively narrow elevational range from 1.25 to 1.64 m above MTL (199 to 229 SWLI; Fig. 4). Vegetation across the transects consists of *C. lyngbyei*, *D. caespitosa*, *D. spicata*, *J. balticus*, and *P. pacifica* on the high marsh. Grain-size analysis shows the relative percent of mud remains relatively constant (92 to 97%) across the transect with the exception of Station 1 (79%). Salinity also displays a relatively constant (16 to 14 ppt) concentration across the transect. TOC_{SOM} shows an increase of >15% organic carbon at Stations 10–13.

We identified 175 species from 55 genera along the transect. The freshwater species L. mutica was present at $\geq 6\%$ abundance at all sampling stations. The brackish species $Navicula\ cincta\ (\leq 12\%)$ and the freshwater species P. $lagerstedtii\ (\leq 15\%)$ are abundant in more than half of the sampling stations.

Hierarchical clustering identified one diatom group at Bone River

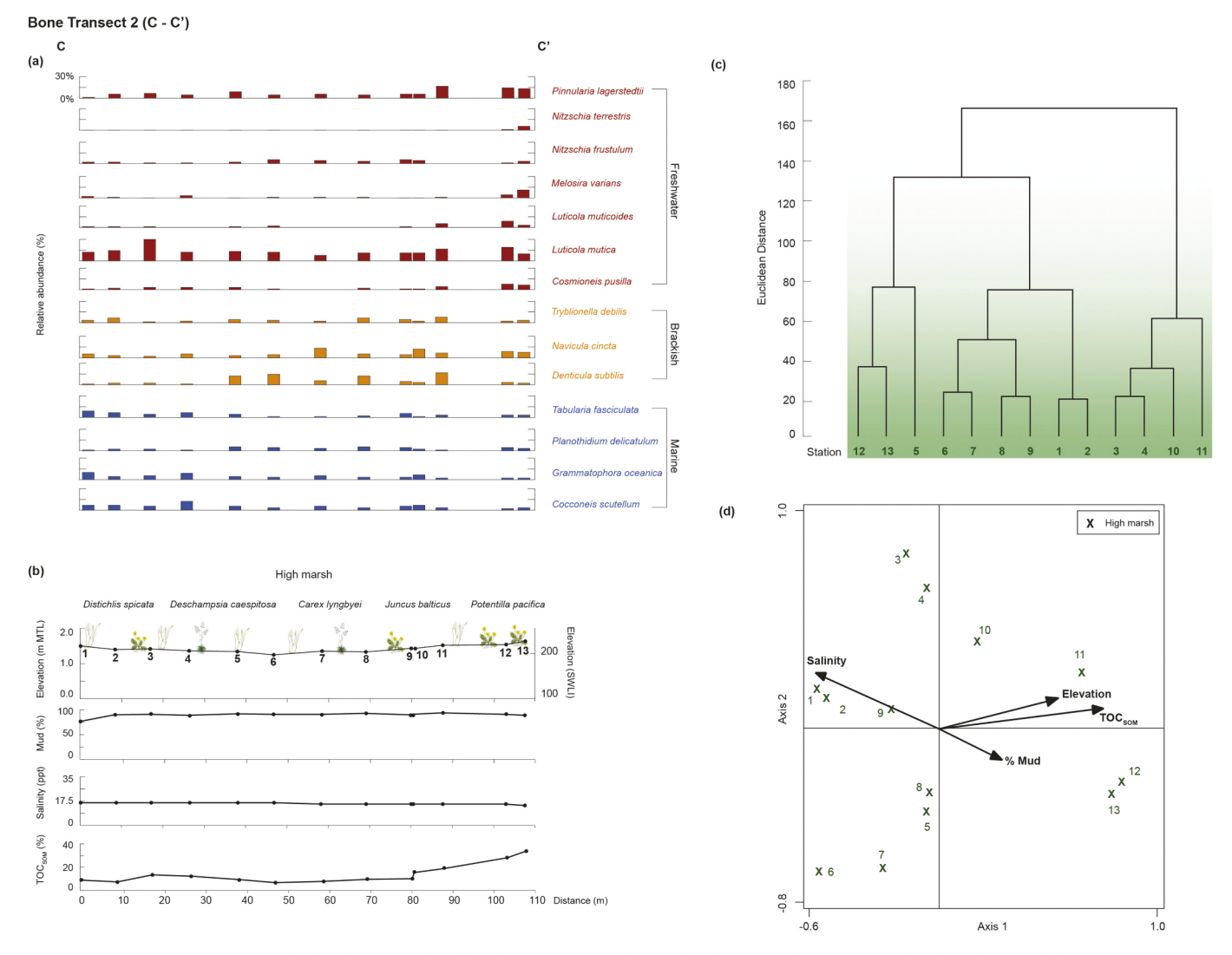


Fig. 4. Bone River Transect 2. (A) The distribution of abundant diatoms (\geq 5% relative abundance in at least one sample) along the sampled transect. Diatoms are separated based on their salinity preferences (blue: marine; red: freshwater). (B) Sampled transect showing the location of the sampling stations and major vascular vegetation separated by zones relative to distance and elevation. The mud fraction, salinity (ppt), and TOC_{SOM} of each sampling station is plotted relative to distance. (C) Results of hierarchical cluster analysis with (D) PCA sample-environment biplot results shown below. Station symbols indicate their sampling location (cross: high marsh). (For interpretation of the references to colour in this figure legend, the reader is referred to the web version of this article.) (For interpretation of the references to colour in this figure legend, the reader is referred to the web version of this article.)

Transect 2 (Fig. 4). PCA produced an Axis 1 with an eigenvalue of 0.22 and an Axis 2 with an eigenvalue of 0.20 that explains 41% of the total variance in the diatom assemblages (Table 1) with 44% explained by the environmental variables (Table 2). Intra-set correlations of environmental variables with axes 1 and 2 show that TOC_{SOM} and elevation are correlated with Axis 1 and that salinity and mud fraction are correlated with both axes 1 and 2 (Fig. 4). Constrained and interactive-forward-selection analyses identified TOC_{SOM} (explains 20% variance) as the major explanatory variable with salinity (explains 10% variance), elevation (explains 8% variance), and mud fraction (explains 6% variance) as minor explanatory variables (Table 2).

4.3. Niawiakum River

4.3.1. Transect 1

Niawiakum River Transect 1 is comprised of 10 sampling stations ranging in elevation from -5.03 to 0.48 m above MTL (-291 to 137 SWLI) across the subtidal (Stations 1-4) to tidal flat (Stations 5-10; Fig. 5). Samples along the transect lacked vascular plants. Grain-size analysis shows that the relative percent of mud ranges from 10 to 65%

and is variable along the transect. Salinity also varies along the transect and ranges from 18 to 35 ppt. ${\rm TOC_{SOM}}$ remains low along the transect, ranging from 0.10 to 0.65%.

We identified 146 species from 55 genera along the transect. In the subtidal we observe marine species (C. scutellum: \leq 16%, P. delicatulum: \leq 23%, and Tabularia fasciculata: \leq 10%). The tidal flat showed an increase in brackish species (Nitzschia filiformis: \leq 12%, Rhopalodia gibberula: \leq 10% and Rhopalodia musculus: 12%). The freshwater species N. frustulum is present in all samples, showing a maximum abundance of 6% in Station 7.

Hierarchical clustering identified two diatom groups along the Nia-wiakum River Transect 1 (Fig. 5). Cluster A consists of Stations 1–8 in which we observe marine species with brackish species in rare abundance. Cluster B consists of Stations 9 and 10 in which we observe brackish species.

PCA produced an Axis 1 with an eigenvalue of 0.37 and an Axis 2 with an eigenvalue of 0.16 that explains 53% of the total variance in the diatom assemblages (Table 1) with 61% explained by the environmental variables (Table 2). Intra-set correlations of environmental variables with axes 1 and 2 show that salinity is correlated with Axis 1 and mud

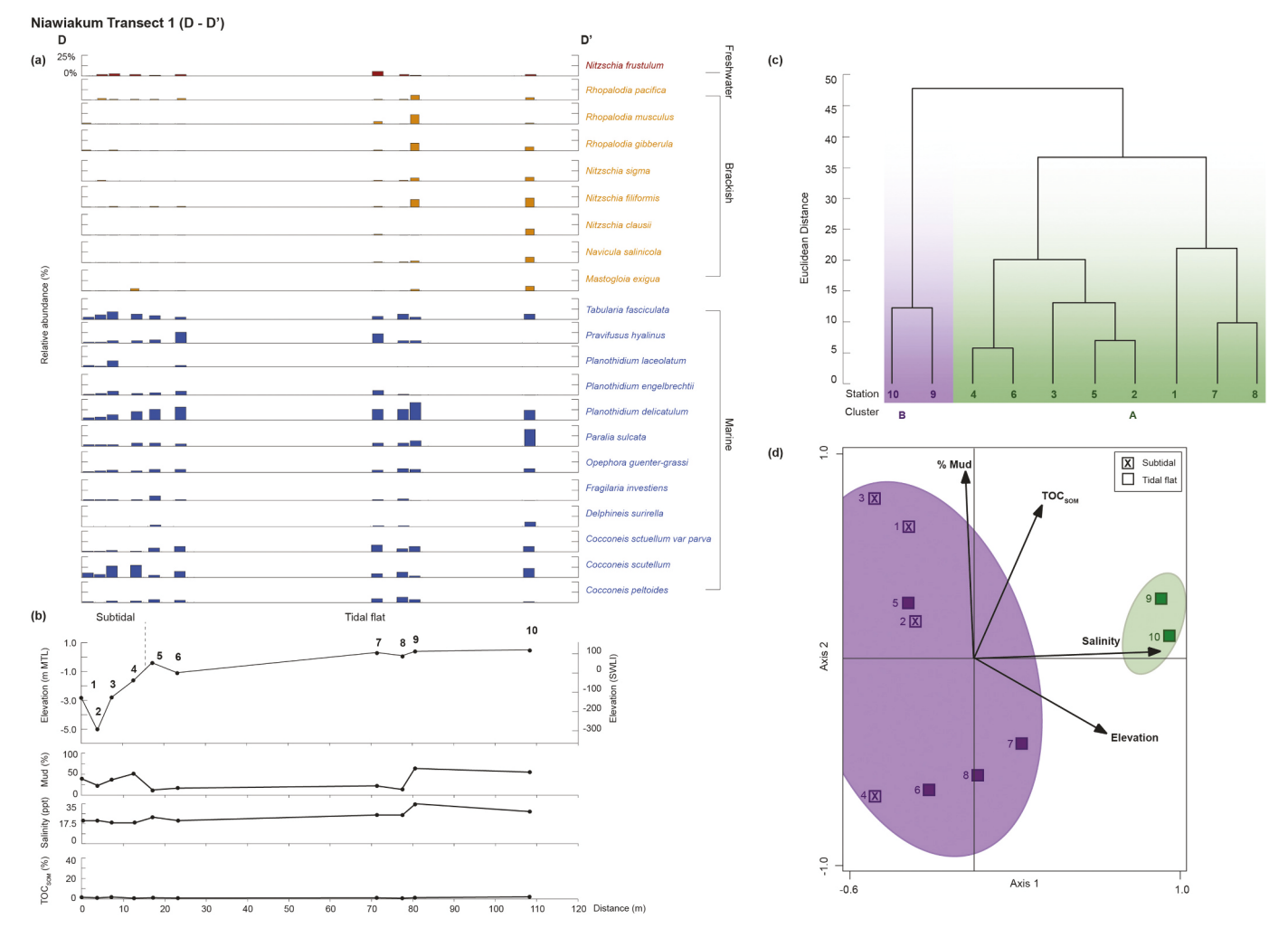


Fig. 5. Niawiakum River Transect 1. (A) The distribution of abundant diatoms (\geq 5% relative abundance in at least one sample) along the sampled transect. Diatoms are separated based on their salinity preferences (blue: marine; yellow: brackish; red: freshwater). (B) Sampled transect showing the location of the sampling stations and major vascular vegetation separated by zones relative to distance and elevation. The mud fraction, salinity (ppt), and TOC_{SOM} of each sampling station is plotted relative to distance. (C) Results of hierarchical cluster analysis with (D) PCA sample-environment biplot results shown below. Station symbols indicate their sampling location (crossed square: subtidal; square: tidal flat). (For interpretation of the references to colour in this figure legend, the reader is referred to the web version of this article.)

fraction is correlated with Axis 2 (Fig. 5). TOC_{SOM} and elevation are correlated with both axes 1 and 2. Constrained and interactive-forward-selection analyses identified salinity (explains 31% variance) as the major explanatory variable with mud fraction (explains 12% variance), TOC_{SOM} (explains 11% variance), and elevation (explains 7% variance) as minor explanatory variables (Table 2).

4.3.2. Transect 2

Niawiakum River Transect 2 is comprised of 20 sampling stations ranging in elevation from -0.80 to 1.79 m above MTL (38 to 239 SWLI) that spans the tidal flat to high marsh (Fig. 6). Vegetation across the transect consists of no vascular plants on the tidal flat (Stations 1-3), *G. maritima, S. virginica, S. alterniflora*, and *T. maritima* on the low marsh (Stations 4-7), and *C. lyngbyei, D. spicata, J. balticus*, and *P. pacifica* on the high marsh (Stations 8-20). Grain-size analysis shows that the relative percent of mud remains >70% at all sampling stations except Station 5 (59% mud). Salinity steadily decreases with increasing elevation from 24 to 12 ppt. TOC_{SOM} increases with elevation from 2 to 32% with the most notable change between Stations 17 and 18.

We identified 206 species from 65 genera along the transect. Marine species (*Paralia sulcata*: \leq 7%, *P. delicatulum*: \leq 6%, and *Thalassiosira pacifica*: \leq 7%) are present in the tidal flat samples. Marine species

(Grammatophora oceanica: \leq 5% and T. pacifica: \leq 7%) as well as freshwater species L. mutica: \leq 7% are present in the low marsh samples. High marsh assemblages are comprised of brackish (N. cincta: \leq 12%) and freshwater species (e.g., C. halophila: \leq 16%, L. mutica: \leq 23%, and P. lagerstedtii: \leq 14%).

Hierarchical clustering identified three diatom groups along the Niawiakum River Transect 2 (Fig. 6). Cluster A consists of tidal flat and low marsh samples from Stations 1–8 with an elevation range of -0.80 to 1.46 m above MTL (38 to 213 SWLI). We observe marine species in Cluster A. Cluster B consists of high marsh samples from Stations 9–18 with an elevation range of 1.55 to 1.71 m above MTL (220 to 233 SWLI). Brackish species dominate in Cluster B. Cluster C consists of high marsh samples from Stations 19–20 with an elevation range of 1.75 to 1.79 m above MTL (236 to 239 SWLI). In contrast to other groups, marine species are rare in Cluster C where we observe freshwater species.

PCA produced an Axis 1 with an eigenvalue of 0.34 and an Axis 2 with an eigenvalue of 0.15 that explains 49% of the total variance in the diatom assemblages (Table 1) with 52% explained by the environmental variables (Table 2). Intra-set correlations of environmental variables with axes 1 and 2 show that elevation is correlated with Axis 1 and that all other environmental variables (salinity, TOC_{SOM}, mud fraction) are correlated with both axes 1 and 2 (Fig. 6). Constrained and interactive-

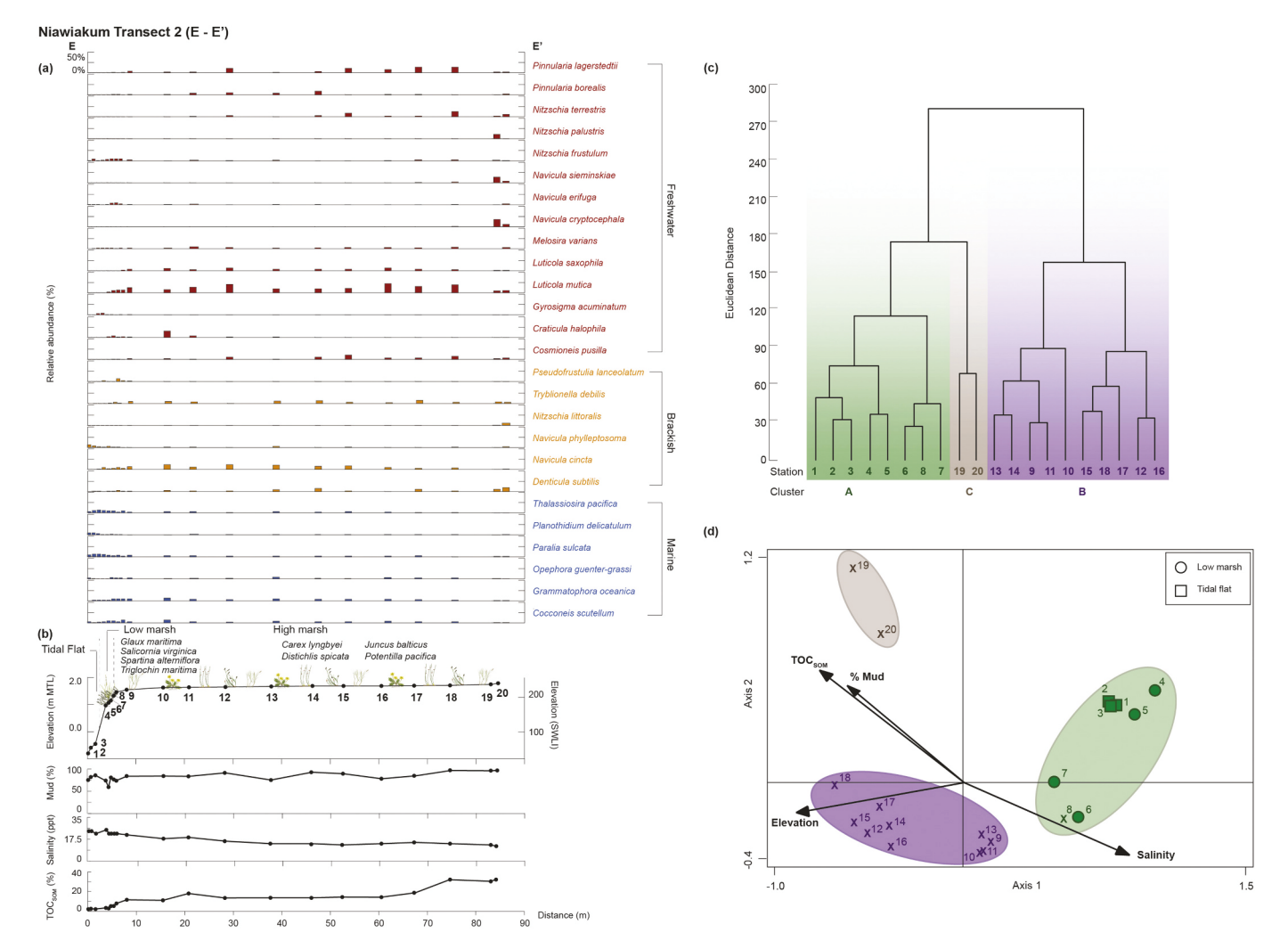


Fig. 6. Niawiakum River Transect 2. (A) The distribution of abundant diatoms (\geq 5% relative abundance in at least one sample) along the sampled transect. Diatoms are separated based on their salinity preferences (blue: marine; yellow: brackish; red: freshwater). (B) Sampled transect showing the location of the sampling stations and major vascular vegetation separated by zones relative to distance and elevation. The mud fraction, salinity (ppt), and TOC_{SOM} of each sampling station is plotted relative to distance. (C) Results of hierarchical cluster analysis with (D) PCA sample-environment biplot results shown below. Station symbols indicate their sampling location (square: tidal flat; circle: low marsh; cross: high marsh). (For interpretation of the references to colour in this figure legend, the reader is referred to the web version of this article.)

forward-selection analyses identified elevation (explains 28% variance) and salinity (explains 14% variance) as major explanatory variables with TOC_{SOM} (explains 6% variance) and mud fraction (explains 4% variance) as minor explanatory variables (Table 2).

4.4. Naselle River

4.4.1. Transect 1

Sampling of Naselle River Transect 1 is comprised of 28 sampling stations ranging in elevation from -0.93 to 2.57 m above MTL (39 to 269 SWLI) that spans the tidal flat to upland (Fig. 7). Vegetation across the transect consists of sparse *Zostera* sp. on the tidal flat (Stations 1–15), *S. virginica* and *T. maritima* on the low marsh (Stations 16–19), and *C. lyngbyei*, *D. caespitosa*, *D. spicata*, *J. balticus*, and *P. pacifica* on the high marsh (Stations 20–27). is comprised of. Sitka spruce (*P. sitchensis*) and Western Crabapple (*P. fusca*) are dominant tree species on the forested upland (Station 28). Grain-size analysis shows the relative percent of mud generally increases with increasing elevation (36 to 99%) throughout the transect with the exception of Station 21 (35%). Salinity generally decreases with increasing elevation from 25 to 8 ppt. TOC_{SOM} increases with elevation from 2 to 36%. We note a drop from 34 to 23%

organic content at Station 27 in the high marsh.

We identified 249 species from 67 genera along the transect. The tidal flat samples contain a mixture of assemblages, likely due to the higher freshwater discharge from the Naselle River, ranging from marine (e.g., *C. scutellum*: \leq 34%) to brackish (e.g., *Staurosirella pinnata*: \leq 10%) as well as freshwater (e.g., *M. varians*: \leq 10%) species. The low marsh includes marine species (*Frustulia linkei*: \leq 14% and *P. sulcata*: \leq 14%). Brackish species *D. subtilis* (\leq 19%) and freshwater species *L. mutica* (\leq 22%) are found in the high marsh. The upland has a mixture of marine (e.g., *Opephora guenter-grassi*: \leq 5%), brackish (e.g., *Tryblionella debilis*: \leq 5%), and freshwater (e.g., *L. mutica*: \leq 12%) species.

Hierarchical clustering identified two diatom groups along the Naselle River Transect 1 (Fig. 7). Cluster A consists of tidal flat, and low marsh samples (Stations 1–17) that range in elevation from -0.93 to 1.84 m above MTL (39 to 221 SWLI). We observe marine and brackish species in Cluster A. Cluster B contains low marsh, high marsh, and upland samples (Stations 18–28) that range in elevation from 1.96 to 2.57 m above MTL (229 to 269 SWLI). In contrast to Cluster A, we observe freshwater species in Cluster B.

PCA produced an Axis 1 with an eigenvalue of 0.36 and an Axis 2 with an eigenvalue of 0.15 that explains 51% of the total variance in the

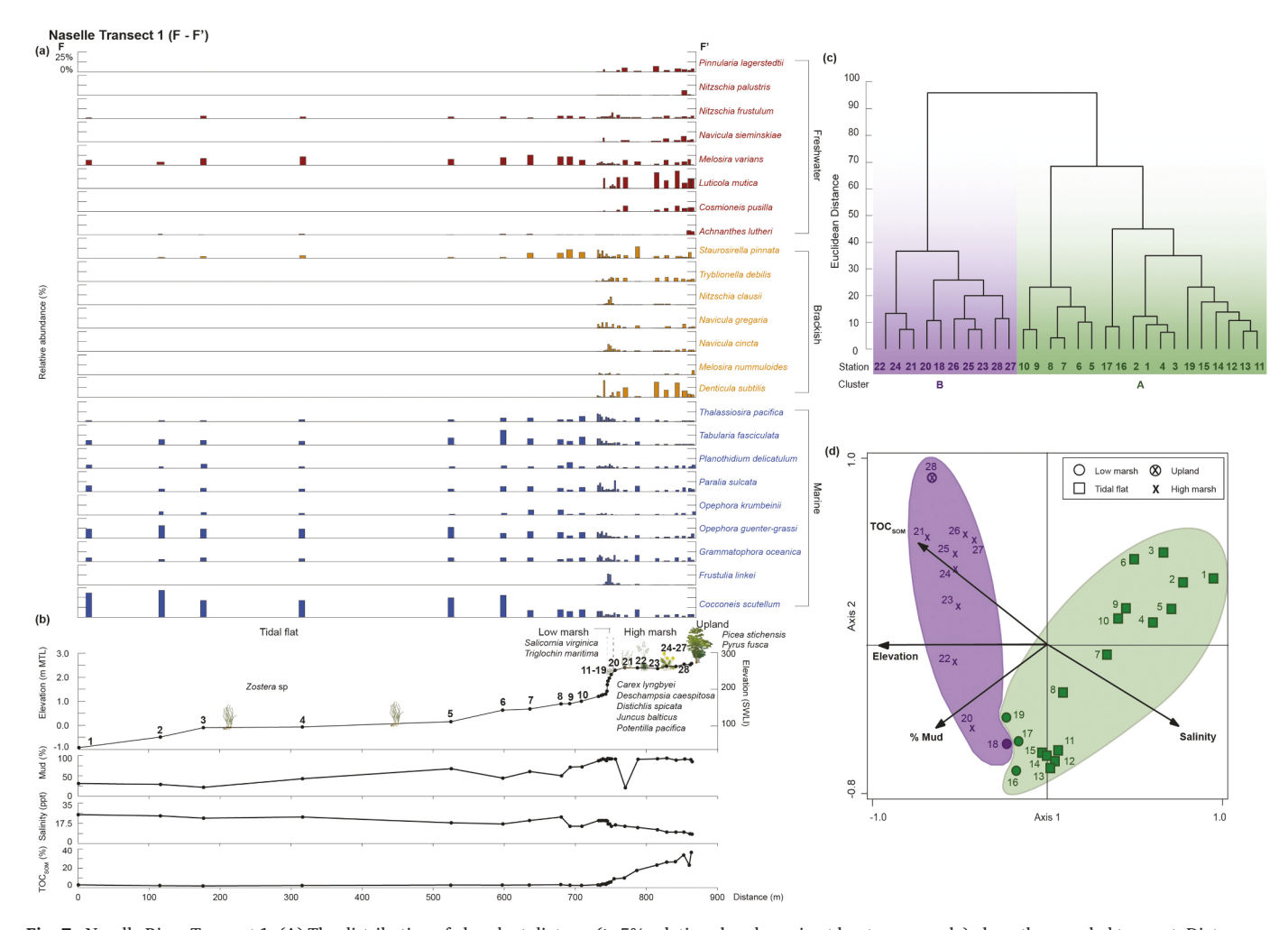


Fig. 7. Naselle River Transect 1. (A) The distribution of abundant diatoms (\geq 5% relative abundance in at least one sample) along the sampled transect. Diatoms are separated based on their salinity preferences (blue: marine; yellow: brackish; red: freshwater). (B) Sampled transect showing the location of the sampling stations and major vascular vegetation separated by zones relative to distance and elevation. The mud fraction, salinity (ppt), and TOC_{SOM} of each sampling station is plotted relative to distance. (C) Results of hierarchical cluster analysis with (D) PCA sample-environment biplot results shown below. Station symbols indicate their sampling location (square: tidal flat; circle: low marsh; cross: high marsh; crossed circle: upland). (For interpretation of the references to colour in this figure legend, the reader is referred to the web version of this article.) (For interpretation of the references to colour in this figure legend, the reader is referred to the web version of this article.)

diatom assemblages (Table 1) with 44% explained by the environmental variables (Table 2). Intra-set correlations of environmental variables with axes 1 and 2 show that elevation is correlated with Axis 1 and salinity, mud fraction, and TOC_{SOM} are correlated with both axes 1 and 2 (Fig. 7). Constrained and interactive-forward-selection analyses identified elevation (explains 27% variance) and salinity (explains 8% variance) as the major explanatory variables with TOC_{SOM} (explains 5% variance) and mud fraction (explains 4% variance) as minor explanatory variables (Table 2).

4.4.2. Transect 2

Sampling of Naselle River Transect 2 is comprised of 7 sampling stations ranging in elevation from 1.67 to 2.65 m above MTL (209 to 273 SWLI) that spans the low and high marsh (Fig. 8). Vegetation across the transect consists of *S. virginica* and *T. maritima* on the low marsh (Stations 1–3) and *C. lyngbyei*, *D. spicata*, and *P. pacifica* on the high marsh (Stations 4–7). Grain-size analysis shows the relative percent of mud remains steady (87 to 93%) throughout the transect. Salinity decreases with increasing elevation from 25 to 2 ppt. TOC_{SOM} increases with elevation from 3 to 22%.

We identified 131 species from 47 genera along the transect. A mixture of marine (e.g., O. guenter-grassi: $\leq 6\%$), brackish (e.g., Navicula

phyllepta: $\leq 12\%$), and freshwater (e.g., N. frustulum: $\leq 14\%$) assemblages are present in the low marsh. The high marsh samples contain ($\leq 18\%$) of freshwater species such as *Cosmioneis pusilla*, L. mutica, Navicula sieminskiae, and Nitzschia terrestris.

Hierarchical clustering identified two diatom groups along Naselle River Transect 2 (Fig. 8). Cluster A consists of low marsh samples (Stations 1–3) that range in elevation from 1.67 to 1.89 m above MTL (209 to 224 SWLI). We observe a mixture of marine, brackish, and freshwater assemblages in Cluster A. Cluster B contains high marsh samples (Stations 4–7) that range in elevation from 2.58 to 2.65 m above MTL (269 to 273 SWLI). We observe freshwater species in Cluster B.

PCA produced an Axis 1 with an eigenvalue of 0.42 and an Axis 2 with an eigenvalue of 0.20 that explains 62% of the total variance in the diatom assemblages (Table 1) with 79% explained by the environmental variables (Table 2). Intra-set correlations of environmental variables with axes 1 and 2 show that mud fraction is correlated with Axis 1 and TOC_{SOM} , elevation, and salinity are correlated with both axes 1 and 2 (Fig. 8). Constrained and interactive-forward-selection analyses identified elevation (explains 39% variance) as the major explanatory variable with TOC_{SOM} , mud fraction, and salinity as minor explanatory variables (explains 21, 10, and 8% variance, respectively; Table 2).

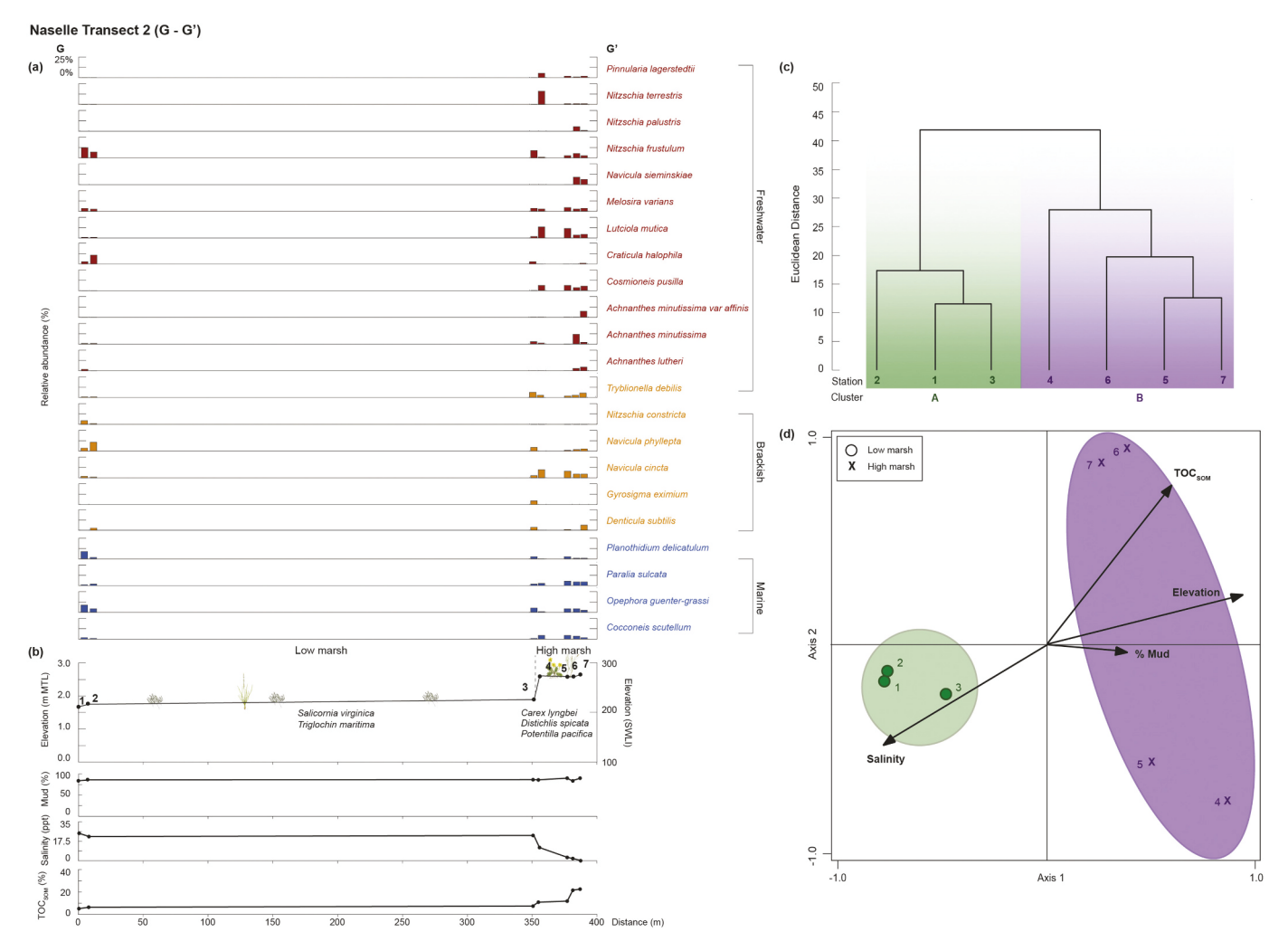


Fig. 8. Naselle River Transect 2. (A) The distribution of abundant diatoms (\geq 5% relative abundance in at least one sample) along the sampled transect. Diatoms are separated based on their salinity preferences (blue: marine; yellow: brackish; red: freshwater). (B) Sampled transect showing the location of the sampling stations and major vascular vegetation separated by zones relative to distance and elevation. The mud fraction, salinity (ppt), and TOC_{SOM} of each sampling station is plotted relative to distance. (C) Results of hierarchical cluster analysis with (D) PCA sample-environment biplot results shown below. Station symbols indicate their sampling location (circle: low marsh; cross: high marsh). (For interpretation of the references to colour in this figure legend, the reader is referred to the web version of this article.)

4.5. Regional dataset

Our combined regional modern diatom dataset is comprised of 104 sampling stations from seven transects that range in elevation from –291 to 273 SWLI. We identified 320 species across 85 genera. Multivariate analysis using hierarchical clustering identified three diatom groups from the regional dataset (Fig. 9):

Cluster A includes the lowest elevation samples of the dataset from Bone River Transect 1, Niawiakum River Transect 1, and Naselle River Transect 1 whose stations range in elevation from -291 to 256 SWLI. Grain-size distributions show a range of 10 to 91% mud. Salinity ranges from 4 to 35 ppt. TOC_{SOM} ranges from 0.38 to 27%. The diatoms of Cluster A are predominantly marine species with a relatively high abundance (5–19%) of the marine species *C. scutellum* var. *parva*, *O. minuta*, and *P. hyalinus* compared to the other clusters.

Cluster B includes (1) high marsh samples from Bone River Transect 2, Niawiakum River Transect 2, Naselle River Transect 1; (2) one of the high marsh samples from Naselle River Transect 2 (Station 4); and one upland sample from Naselle River Transect 1 (Station 28). The elevation range for this group of samples is from 186 to 271 SWLI. Grain-size distributions show a range of 35 to 99% mud with a salinity range of 8 to 20 ppt. TOC_{SOM} ranges from 4 to 36%. The diatoms of Cluster B are a

mix of dominantly brackish and freshwater species with a relatively high abundance of the freshwater species *C. pusilla* and *N. terrestris* compared to the other clusters.

Cluster C consists of samples from all 7 transects whose stations range in elevation from 38 to 273 SWLI and includes the highest elevation samples. Grain-size distributions have a large range from 31 to 100% mud with a salinity range from 2 to 35 ppt. TOC_{SOM} ranges from 1 to 30%. The diatoms of Cluster C are a mix of marine (e.g., *G. oceanica* and *T. pacifica*), brackish (e.g., *S. pinnata* and *N. gregaria*), and freshwater (e.g., *C. halophila*) species.

PCA produced an Axis 1 with an eigenvalue of 0.21 and an Axis 2 with an eigenvalue of 0.09 that explains 31% of the total variance in the diatom assemblages (Table 1) with 28% explained by the environmental variables (Table 2). The intra-set correlations of environmental variables with axes 1 and 2 show that mud fraction, TOC_{SOM} , salinity, and elevation are correlated with Axis 1 and site is correlated with Axis 2 (Fig. 9). Constrained and interactive-forward-selection analysis identified mud fraction (explains 12% variance), TOC_{SOM} (explains 6% variance), salinity (explains 10% variance), elevation (explains 9% variance), and site (explains 5% variance) as major explanatory variables (Table 2). A boxplot showing the distribution of elevation (SWLI) for the clustered sampling stations show the median of each cluster

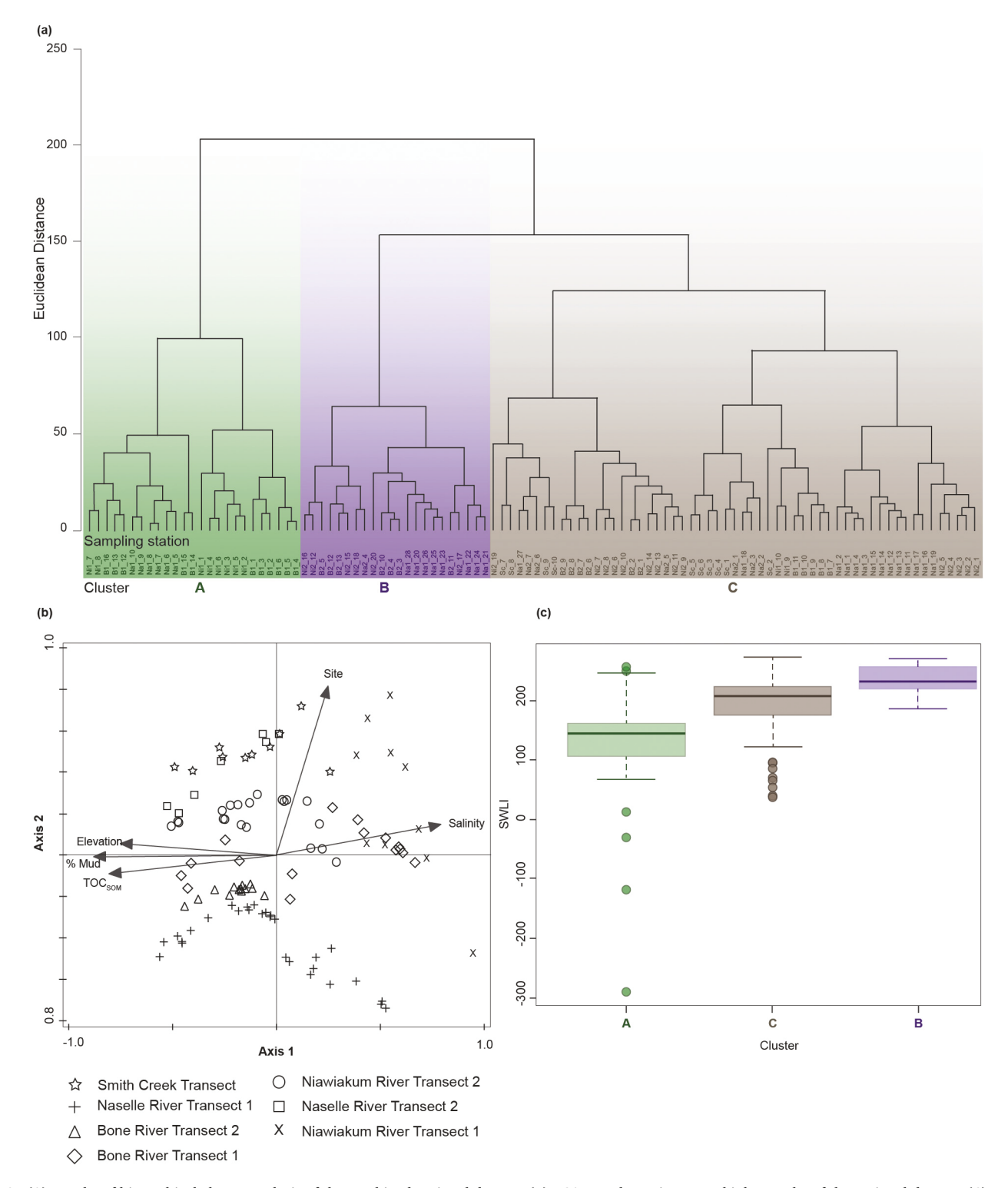


Fig. 9. (A) Results of hierarchical cluster analysis of the combined regional dataset. (B) PCA sample-environment biplot results of the regional dataset. (C) Boxplot showing the distribution of elevation (SWLI) for clustered sampling stations.

plotted separately despite overlapping elevation ranges (Fig. 9). Cluster A displays the lowest elevation median and widest range of outliers compared to Cluster B and C. In contrast, Cluster B displays the highest elevation median and narrowest range with no outliers. Cluster C shows outliers at lower elevations and a median value between that of Cluster A and B.

Weighted averaging results from 65 species show that the elevation optima of our regional dataset span multiple environments across

elevation (88 to 251 SWLI) and that species displayed varying elevation tolerances (Fig. 10). Marine and brackish species dominate elevations lower than MHHW (elevation optima <200 SWLI), whereas freshwater species dominate above MHHW (elevation optima >200 SWLI). Marine and brackish species display a wider elevation tolerance across the intertidal compared to freshwater species. Of the 24 species with an elevation tolerance of less than 50 SWLI, 14 are freshwater species. Above MHHW, the freshwater species *N. cryptocephala* (optima 238

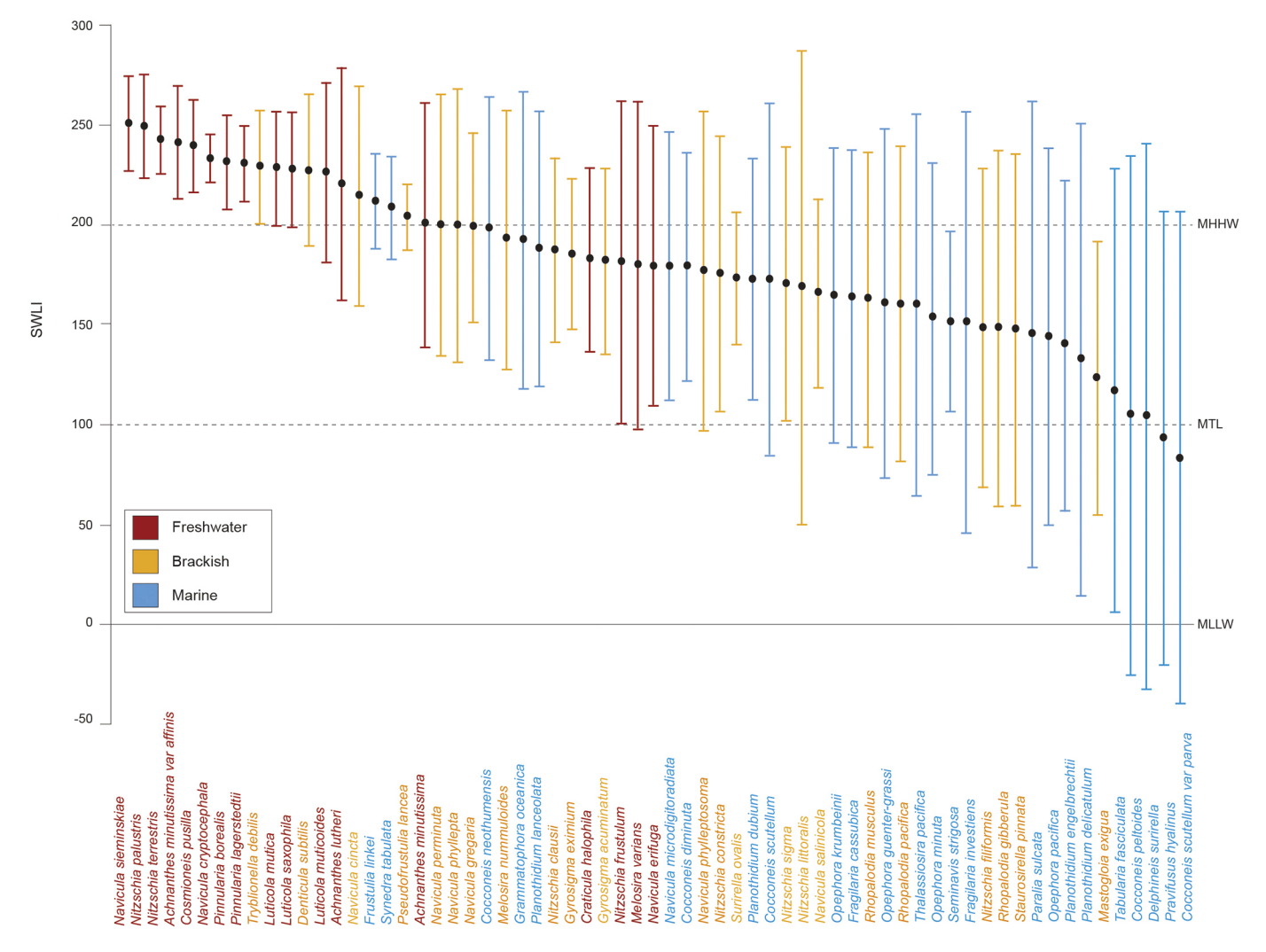


Fig. 10. Results of weighted averaging with optimal elevation (circles) and elevation tolerance (brackets) of abundant diatom species (\geq 5% relative abundance in one sample). Diatom labels are colour coded based on salinity preferences (blue: marine; yellow: brackish; red: freshwater). (For interpretation of the references to colour in this figure legend, the reader is referred to the web version of this article.) (For interpretation of the references to colour in this figure legend, the reader is referred to the web version of this article.)

SWLI), *N. terrestris* (optima 243 SWLI), and *P. lagerstedtii* (optima 231 SWLI) displayed the narrowest elevation tolerances of all species ranging from 15 to 19 SWLI. Between MHWW and MTL the brackish species *G. eximium* (optima 185 SWLI) and *Surirella ovalis* (optima 174 SWLI) showed elevation tolerances of 34 and 38 SWLI, respectively. Of the 9 species with an elevation tolerance greater than 100 SWLI, 8 are marine and 1 is brackish. Below MTL, the marine species *P. hyalinus* (optima 93 SWLI) and *C. scutellum var. parva* (87 SWLI) showed a wide elevation tolerance (113 and 121 SWLI, respectively).

5. Discussion

5.1. Vertical zonation of diatom distributions in Willapa Bay

Consistent with studies in Cascadia (e.g., Nelson and Kashima, 1993; Hemphill-Haley, 1995a, 1995b; Sherrod, 1999) and elsewhere (e.g., Admiraal, 1977; Zong and Horton, 1998; Sawai, 2001; Zong et al., 2003; Shennan and Hamilton, 2006; Garrett et al., 2013; Watcham et al., 2013), five sites (Smith Creek Transect, Bone River Transect 1, Niawiakum River Transect 2, Naselle River Transect 1, and Naselle River Transect 2) displayed a vertical zonation of diatom assemblages. Vertical zonation of diatom assemblages in Willapa Bay were also observed by Hemphill-Haley (1995b) who used factor analysis to identify three

distinct clusters of diatom assemblages that separated across elevation at the Niawiakum River. Two sites (Bone River Transect 2, and Niawiakum River Transect 1) do not display a vertical zonation, however, their diatom assemblages do distinguish the subtidal/tidal flat and/or high marsh/upland environments.

The subtidal environments of Niawiakum River Transect 1 and the tidal flats of Smith Creek Transect, Bone River Transect 1, Niawiakum River Transect 2, and Naselle River Transect 1 are characterized by coarser (lower mud fraction) grain-size, lower organic content, and higher salinity. In these environments, we observe epiphytic (attachment to aquatic plants) and epipsammic (attachment to sand) marinebrackish species such as G. oceanica, O. guenter-grassi, and T. fasciculata. Sawai et al. (2016) noted similar species (e.g., epiphytic species T. fasciculata) on tidal flats and low marsh environments along the Oregon coast. Hemphill-Haley (1995b) also found a vertical zonation of diatom assemblages along two transects at the Niawiakum River, observing similar species (e.g., T. fasciculata and G. oceanica) as indicative of tidal flats, but also noted their wide distribution along the subtidal and tidal flat. Species in our subtidal samples from Niawiakum River Transect 1 also displayed a lack of distinct zonation, showing similar distribution and relative abundance with species in tidal flat samples (Fig. 5).

Low marshes are characterized by finer (higher mud fraction) grain-

size, slightly increased TOC_{SOM}, and slightly decreased salinity relative to tidal flats. The changing environmental conditions from the tidal flat to low marsh coincide with a decrease in marine species (e.g., Nelson and Kashima, 1993; Hemphill-Haley, 1995b; Sherrod, 1999) and the appearance of brackish species such as *G. eximium* and *N. gregaria* (e.g., Sawai et al., 2016). We also observe marine (e.g., *O. pacifica*) and freshwater (e.g., *N. frustulum*) diatom species, which tolerate a wide range of intertidal environments and can be found in high abundances in low marshes at Cascadia (e.g., Hemphill-Haley, 1995b; Sherrod, 1999) and the U.K. (Zong and Horton, 1998). Hemphill-Haley (1995b) identified species such as *F. linkei*, *G. eximium*, and *M. exigua* as indicative of the low marsh. Although we do find *F. linkei* at the Naselle River Transect 1 and *M. exigua* at Smith Creek Transect and Niawiakum River Transect 1, they are not found in other transects.

The high marsh and upland are characterized by muddy substrates, high TOC_{SOM}, and low salinity (with higher elevations comes lower flooding frequency). We observe aerophilous (tolerant of temporarily dry conditions) and freshwater tolerant species such as *C. pusilla*, *L. mutica*, *N. cincta*, *N. terrestris*, and *P. lagerstedtii*. These species are indicative of the high marsh environment in estuaries along the coasts of Oregon and Washington, and in Puget Sound (Sherrod, 1999; Hemphill-Haley, 1995b; Sawai et al., 2016). Hemphill-Haley (1995b) found similar freshwater species (e.g., *N. terrestris*) in the high marsh to upland transition of her Lower Niawiakum River transect. A regional diatom distribution study by Sawai et al. (2016) included 12 high marsh samples at the Niawiakum River with a dominance of the freshwater species *C. pusilla*, *L. mutica*, and *Nitzschia brevissima*.

5.2. Environmental variables and diatom zonation

Our study shows that no single variable consistently explains variations in diatom assemblages at every site because diatoms exhibit a complex relationship with environmental variables (Desianti et al., 2019). In a regional diatom distribution study of 11 wetland sites of the Oregon (10 sites) and Washington (Niawiakum River) coastline (Sawai et al., 2016), dominant environmental controls varied by site and were attributed to differences in the physiographic features of the individual estuaries.

We show that elevation, salinity, and substrate (mud fraction and TOC_{SOM}) are variables affecting diatom variability along our transects (Table 2). Similar studies at Cascadia show a strong relationship with elevation and other environmental variables correlated with tidal exposure (e.g., Hemphill-Haley, 1995b; Nelson and Kashima, 1993) such as salinity (e.g., McIntire, 1978; Sherrod, 1999) and substrate (grain-size and organic content; e.g., Amspoker and McIntire, 1978; Sawai et al., 2016). Elevation is the dominant environmental variable at Bone River Transect 1 (35% of variation), Niawiakum River Transect 2 (28% of variation), Naselle Transect 1 (27% of variation), and Naselle Transect 2 (39% of variation) where the diatoms display a distinct vertical zonation (Table 2). The importance of elevation as an environmental control on modern diatom distributions is due to the covarying relationship between elevation and other environmental variables, such as the frequency and duration of tidal flooding/exposure, that influence diatom distributions (e.g., Nelson and Kashima, 1993; Zong and Horton, 1999; Sawai et al., 2004a, 2004b).

Salinity is shown to be the dominant environmental variable at the Niawiakum River Transect 1 (31% of variance), which is consistent with other studies that show salinity to be a major driver of diatom variability (e.g., Hendy, 1964; Amspoker and McIntire, 1978; Zong, 1997a; Hassan et al., 2009). Sherrod (1999), observing an inverse relationship between salinity and elevation, used canonical correspondence analysis to show that changes in the modern diatom assemblage distribution in a Puget Sound (Washington, USA) salt marsh was primarily driven by salinity with elevation as the secondary control. The importance of salinity as a major variable is further highlighted by a study of modern diatom distributions from Yaquina Estuary, Oregon (USA) that found large

differences in diatom assemblages between adjacent sampling stations as a result of changes in salinity along the sampled gradient (McIntire, 1978).

Substrate is shown to be the dominant environmental variable at Smith Creek Transect (32% of variance) and Bone River Transect 2 (20% of variance). Substrate can influence the abundance and distribution of intertidal diatoms (e.g., Kosugi, 1987; Vos and de Wolf, 1993) because in tidal marsh settings substrate will often co-vary with elevation as grainsize shifts from coarser sediments in the tidal flat to finer grained, silt-dominated sediments with increasing elevation (e.g., Zong and Horton, 1999; Sawai et al., 2004a; Yang et al., 2008). Similarly, organic content has been shown to rise with increasing elevation (e.g., Shennan et al., 1994; Zong and Horton, 1999; Sawai et al., 2004a). Sawai et al. (2016) found loss-on-ignition (% organic matter) explained the most variance at 6 out of 10 estuaries of the Oregon coastline as well as at the Niawiakum River. Diatom sensitivity to organic content, which is an indicator of trophic conditions, is well established and forms the basis of the saprobic diatom classification system (Sladecek, 1986).

Our regional analysis of the combined diatom dataset suggests that the environmental variables co-vary along an elevation gradient. A regional study of intertidal diatom distributions and their environmental variables from six sites of the British coastline also observed that the environmental variables (clay-silt-sand fraction, organic content, vegetation cover, and elevation) varied along an elevation gradient (Zong and Horton, 1998). The regional analysis show that 28% of the diatom variance can be explained by the measured environmental variables (elevation, mud fraction, TOCSOM, salinity, and site) although higher rates of explanation are found at individual transects (Table 2). The percentage of explained variation in our study is consistent with other diatom studies due to the large sample size and many zero values inherent in biological datasets (Gasse et al., 1995; Jones and Juggins, 1995; Zong and Horton, 1998; Sawai et al., 2016). The unexplained variance may be due to environmental variables that were not analyzed in this study. For example, diatom assemblages and their growth rate (e. g., Hutchins and Bruland, 1998; Sarthou et al., 2005) are influenced by light intensity (e.g., Castenholz, 1961; McIntire, 1978; Admiraal and Peletier, 1980), temperature (e.g., Amspoker and McIntire, 1978; McIntire, 1978), and nutrient concentrations (e.g., Peletier, 1996; Lange et al., 2011).

5.3. Implications of diatom distributions for sea-level reconstructions at Cascadia

Over the past 30 years, Willapa Bay has been a focus of RSL studies seeking to estimate amounts of land-level change during past megathrust earthquakes as a way of inferring earthquake magnitudes (e.g., Atwater, 1987; Hemphill-Haley, 1995a; Atwater and Hemphill-Haley, 1997; Sabean, 2004). Microfossil-based sea-level reconstructions have been used in Cascadia to provide quantitative estimates of RSL rise during earthquakes with sample-specific errors (e.g., Guilbault et al., 1996; Sawai et al., 2004a, 2004b; Nelson et al., 2008; Hawkes et al., 2010; Garrett et al., 2013; Milker et al., 2016; Hocking et al., 2017 Kemp et al., 2018; Padgett et al., 2021). Microfossil-based sea-level reconstructions rely on the empirically derived relationship between present-day species of microorganisms and tidal exposure to infer estimates of RSL change (e.g., Shennan et al., 1996; Sherrod, 1999; Sawai et al., 2004a, 2004b; Hawkes et al., 2010; Engelhart et al., 2013; Kemp et al., 2018). Our regional study provides an important dataset that builds upon previous modern diatom distribution studies in the Niawiakum River, Willapa Bay (Hemphill-Haley, 1995b; Sawai et al., 2016) by offering additional observations regarding species abundance and distribution from multiple tidal wetland sites that can be used to inform RSL reconstructions in Willapa Bay:

Diatom species with narrow (< 50 SWLI), or distinct, elevation tolerances can serve as indicator species of specific environments (e.g., Hemphill-Haley, 1995b; Tornés et al., 2007; Desianti et al., 2019). We

suggest that freshwater species (e.g., C. pusilla, L. mutica, N. terrestris, and P. lagerstedtii), which displayed narrow elevation tolerances, are indicator species for high marsh or upland environments. Similarly, brackish species (e.g., G. eximium and S. ovalis), which displayed narrow elevation tolerances, are indicator species for low marsh environments. Importantly, these species are commonly identified in intertidal stratigraphic sequences of megathrust earthquakes from Washington (e.g., Hemphill-Haley, 1995a; Shennan et al., 1996) and Oregon (e.g., Nelson et al., 2008; Graehl et al., 2014). Future RSL reconstructions could focus on identifying species with well-constrained modern distributions that can be applied to downcore fossil assemblages to distinguish past intertidal environments. Furthermore, observations of indicator species can be extended to inform the development of other, proxy-based RSL reconstruction models, such as the foraminifera-based Bayesian transfer function, by applying the presence of diatom indicator species as a secondary proxy (Kemp et al., 2018).

Additional work is needed to examine the potential impact of species with allochthonous components on RSL reconstructions. We note that allochthonous (transported) species or species with allochthonous components such as *C. scutellum*, *M. varians*, *P. sulcata*, and *P. delicatulum* were found across multiple environments with an elevation tolerance ranging from 81 to 117 SWLI (Fig. 10). These species are often found in intertidal environments beyond their habitat and thus may be less useful in RSL reconstructions (Hemphill-Haley, 1995a; Sawai, 2001; Dura et al., 2016b; Sawai et al., 2016). For this reason, Sawai et al. (2004a) removed *P. sulcata* and the p-valve (allochthonous component) of *C. scutellum* in the development of a diatom transfer function along the Pacific coast of eastern Hokkaido, Japan. Future RSL reconstructions at Willapa Bay may benefit from examining the performance of different transfer function models that include or remove allochthonous species.

The collection of a regional modern diatom dataset is crucial to developing a robust understanding of diatom variability. The sitespecific variability of our dataset illustrates the importance of collecting a modern dataset with a large sample size that covers a broad range of modern depositional environments in order to provide modern analogs that reflect the variability of diatoms in fossil cores (e.g., Gehrels et al., 2001; Barlow et al., 2013; Watcham et al., 2013). Our results showed species with elevation distributions that vary by site or species found in relatively high abundance at one site that are not found regionally throughout Willapa Bay. For example, the brackish species S. pinnata was found (> 5% abundance) throughout Naselle River Transect 1 but was not found in other transects. Although local datasets have been applied to reconstruct RSL change (e.g., Woodroffe and Long, 2010), our results align with studies showing that regional datasets provide a more comprehensive set of analogous environments from which RSL reconstructions are possible (e.g., Horton and Edwards, 2005; Watcham et al., 2013; Hocking et al., 2017; Kemp et al., 2018).

6. Conclusion

We assess the intertidal distribution of modern diatoms along seven transects from Willapa Bay, Washington. Hierarchical clustering and ordination of individual and regional datasets identified floral zones with differing environmental variable controls:

1. On the subtidal/tidal flat, which is associated with a higher sand fraction, low TOC_{SOM}, and high salinity, we see epiphytic and epipsammic marine species (e.g., *G. oceanica, O. pacifica,* and *T. fasciculata*). Transitioning from the tidal flat to low marsh resulted in a higher mud fraction, slightly increased TOC_{SOM}, and lower salinity where species that are tolerant of a wider salinity range (e.g., *G. eximium* and *N. gregaria*) were found. In the high marsh/upland, which is associated with a dominance of mud, high TOC_{SOM}, and low salinity, we observe aerophilous freshwater species (e.g., *N. terrestris*, and *P. lagertedtii*).

- 2. At four of seven of our transects, diatom assemblages showed a distinct separation of the tidal flat, low marsh, and high marsh: three diatom groups were identified at Bone River Transect 1, Niawiakum River Transect 2, Naselle River Transect 1, and Naselle River Transect 2 which displayed a vertical zonation with elevation (explains 35%, 28%, 27%, and 39% of the variance, respectively) as the major environmental control.
- Different environmental controls drove diatom variability at Smith Creek Transect (TOC_{SOM}: 32% variance), Bone River Transect 2 (TOC_{SOM}: 20% variance), and Niawiakum River Transect 1 (salinity: 31% variance).
- 4. PCA sample-environment biplot results of the regional dataset show the orientation of the environmental vectors elevation, salinity, and substrate are oriented along Axis 1, suggesting that the environmental variables along Axis 1 co-vary along an elevation gradient and that elevation is a key driver of regional diatom variability in Willana Bay.
- 5. Weighted averaging of our regional dataset shows elevation optima and tolerance that cover a broad range of environments across the intertidal zones (251 to 88 SWLI), indicating its applicability in RSL reconstructions. Marine and brackish species display a wider elevation tolerance across the intertidal zone compared to freshwater species.

Our findings show that despite the site-specific variability of our modern diatom distribution, the regional dataset provides an important dataset that can be used to reconstruct RSL in Willapa Bay. Considerations for future RSL reconstructions include exploiting indicator species with narrow or distinct elevation tolerances and examining the impact of allochthonous species on RSL reconstructions. Furthermore, the study highlights the continued importance of collecting a regional dataset to provide a variety of environments from which to inform RSL reconstructions.

Author statement

All authors contributed to the acquisition of data and revising the manuscript critically for important intellectual content. IH wrote the first draft of the manuscript. IH, BPH, ADH, and SEE designed the research approach. IH, ADH, and RJO III conducted analysis of the data.

Declaration of Competing Interest

The authors declare that they have no known competing financial interests or personal relationships that could have appeared to influence the work reported in this paper.

Acknowledgements

IH was supported by the National Science Foundation EAR 1952740 and EAR 1419824 to BPH. Project support by EAR 1419846 (ADH) and EAR 1419844 (SEE). TD was supported by EAR 1624795. BPH is supported by the Earth Observatory of Singapore via its funding from the Singapore Ministry of Education Academic Research Fund MOE2019-T3-1-004, the National Research Foundation Singapore, and the Singapore Ministry of Education under the Research Centers of Excellence initiative. The authors acknowledge the use of facilities, plus the scientific and technical assistance of the instrument staff at the M.J. Murdock Charitable Trust Multidisciplinary Research Laboratory, Central Washington University, USA, a facility partially funded by the M.J. Murdock Charitable Trust. We thank Editor Xavier Crosta for overseeing review of the manuscript and two anonymous reviewers for their help in improving the manuscript. We thank Alan Nelson and Eileen Hemphill-Haley for providing helpful comments to an earlier draft of this paper. This paper is a contribution to International Geoscience Programme (IGCP) Project 639 "Sea-Level Changes from Minutes to Millennia". This work comprises Earth Observatory of Singapore contribution no. 395.

References

- Abdi, H., Williams, L.J., 2010. Principal component analysis. Wiley Interdiscip. Rev. Comp. Stat. 2 (4), 433–459.
- Admiraal, W., 1977. Influence of light and temperature on the growth rate of estuarine benthic diatoms in culture. Mar. Biol. 39, 1–9.
- Admiraal, W., 1984. The ecology of estuarine sediment-inhabiting diatoms. Prog. Phycol. Res. 3, 269–322.
- Admiraal, W., Peletier, H., 1980. Influence of seasonal variations of temperature and light on the growth rate of cultures and natural populations of intertidal diatoms. Mar. Ecol. Prog. Ser. 2 (35–43).
- Amspoker, M.C., McIntire, C.D., 1978. Distribution of intertidal diatoms assoicated with sediments in Yaquina Bay Estuary, Oregon 1, 2. J. Phycol. 14 (4), 387–395.
- Atwater, B.F., 1987. Evidence for great holocene earthquakes along the outer coast of Washington State. Science 236 (4804), 942–944.
- Atwater, B.F., Hemphill-Haley, E., 1997. Recurrence intervals for great earthquakes of the past 3,500 years at northeastern Willapa Bay, Washington. In: U.S. Geological Survey Professional Paper 1576, p. 108. https://pubs.er.usgs.gov/publication/pp 1576.
- Banas, N., Hickey, B., 2005. Mapping exchange and residence time in a model of Willapa Bay, Washington, a branching, macrotidal estuary. J. Geophys. Res. Oceans 110 (C11).
- Barlow, N.L.M., Shennan, I., Long, A.J., Gehrels, W.R., Saher, M.H., Woodroffe, S.A., Hillier, C., 2013. Salt marshes as late Holocene tide gauges. Glob. Planet. Chang. 106, 90–110.
- Battarbee, R.W., Jones, V.J., Flower, R.J., Cameron, N.G., Bennion, H., Carvalho, L., Juggins, S., 2002. Diatoms, Tracking Environmental Change using Lake Sediments. Springer, pp. 155–202.
- Birks, H.J.B., 1995. Quantitative palaeoenvironmental reconstructions. In: Maddy, D., Brew, J.S. (Eds.), Statistical Modelling of Quaternary Science Data. Quaternary Research Association, London, pp. 161–254.
- Birks, H.J.B., Braak, C.J.F.T., Line, J.M., Juggins, S., Stevenson, A.C., Battarbee, R.W., Mason, B.J., Renberg, I., Talling, J.F., 1990. Diatoms and pH reconstruction: Philosophical transactions of the Royal Society of London. B, Biol. Sci. 327 (1240), 263–278
- Brader, M., Garrett, E., Melnick, D., Shennan, I., 2020. Sensitivity of tidal marshes as recorders of major megathrust earthquakes: constraints from the 25 December 2016 Mw 7.6 Chiloe earthquake, Chile. J. Quat. Sci. https://doi.org/10.1002/jqs.3323.
- Castenholz, R.W., 1961. The effect of grazing on marine littoral diatom populations. Ecology 42 (4), 783–794.
- Conger, P.S., 1951. Diatoms. Sci. Mon. 73, 315-323.
- Cooke, S.S., 1997. A Field Guide to the Common Wetland Plants of Western Washington & Northwestern Oregon. Seattle Audubon Society.
- Darienzo, M.E., Peterson, C.D., 1990. Episodic tectonic subsidence of late Holocene salt marshes, northern Oregon central Cascadia margin. Tectonics 9 (1), 1–22.
- Denys, L., 1991/1992. A check-list of the diatoms in the Holocene deposits of the western Belgian coastal plain with a survey of their apparent ecological requirements. I. Introduction, ecological code and complete list. Geol. Survey Belgium. 246, 1–41.
- Desianti, N., Enache, M.D., Griffiths, M., Biskup, K., Dege, A., DaSilva, M., Millermann, D., Lippincott, L., Watson, E., Gray, A., Nikitina, D., Potapova, M., 2019. The Potential and Limitations of Diatoms as Environmental Indicators in Mid-Atlantic Coastal. Estuaries and Coasts, Wetlands. https://doi.org/10.1007/s12237-019-00603-4.
- Donato, S., Reinhardt, E., Boyce, J., Pilarczyk, J., Jupp, B., 2009. Particle-size distribution of inferred tsunami deposits in Sur Lagoon, Sultanate of Oman. Mar. Geol. 257 (1–4), 54–64.
- Dura, T., Engelhart, S.E., Vacchi, M., Horton, B.P., Kopp, R.E., Peltier, W.R., Bradley, S., 2016a. The role of holocene relative sea-level change in preserving records of subduction zone earthquakes. Curr. Clim. Change Rep. 2, 86–100. https://doi.org/ 10.1007/s40641-016-0041-y.
- Dura, T., Hemphill-Haley, E., Sawai, Y., Horton, B.P., 2016b. The application of diatoms to reconstruct the history of subduction zone earthquakes and tsunamis. Earth Sci. Rev. 152, 181–197.
- Emmett, R., Llansó, R., Newton, J., Thom, R., Hornberger, M., Morgan, C., Levings, C., Copping, A., Fishman, P., 2000. Geographic signatures of North American West Coast estuaries. Estuaries 23 (6), 765–792.
- Engelhart, S.E., Horton, B.P., Nelson, A.R., Hawkes, A.D., Witter, R.C., Wang, K., Wang, P.-L., Vane, C.H., 2013. Testing the use of microfossils to reconstruct great earthquakes at Cascadia. Geology 41 (10), 1067–1070.
- Engelhart, S.E., Vacchi, M., Horton, B.P., Nelson, A.R., Kopp, R.E., 2015. A Sea Level Database for the Central Pacific coast of North America. Quat. Sci. Rev. 113, 78–92.
- Fritz, S.C., Juggins, S., Battarbee, R.W., Engstrom, D.R., 1991. Reconstruction of past changes in salinity and climate using a diatom-based transfer function. Nature 352 (6337), 706–708.
- Garrett, E., Shennan, I., Watcham, E., Woodroffe, S., 2013. Reconstructing paleoseismic deformation, 1: modern analogues from the 1960 and 2010 Chilean great earthquakes. Quat. Sci. Rev. 75, 11–21.
- Gasse, F., Juggins, S., Khelifa, L.B., 1995. Diatom-based transfer functions for inferring past hydrochemical characteristics of African lakes. Palaeogeogr. Palaeoclimatol. Palaeoecol. 117, 31–54.
- Gehrels, W.R., Roe, H.M., Charman, D.J., 2001. Foraminifera, testate amoebae and diatoms as sea-level indicators in UK saltmarshes: a quantitative multiproxy approach. J. Quat. Sci. Pub. Quat. Res. Assoc. 16 (3), 201–220.

- Gingras, M.K., Pemberton, S.G., Saunders, T., Clifton, H.E., 1999. The ichnology of modern and pleistocene brackish-Water deposits at Willapa Bay, Washington: variability in estuarine settings. PALAIOS 14, 352–374.
- Graehl, N.A., Kelsey, G.M., Witter, R.C., Hemphill-Haley, E., Engelhart, S.E., 2014. Stratigraphic and microfossil evidence for a 4500-year history of Cascadia subduction zone earthquakes and tsunamis at Yaquina River estuary, Oregon, USA. GSA Bull. 127. 211–226.
- Guilbault, J.-P., Clague, J.J., Lapointe, M., 1996. Foraminiferal evidence for the amount of coseismic subsidence during a late Holocene earthquake on Vancouver Island, west coast of Canada. Quat. Sci. Rev. 15 (8–9), 913–937.
- Haggart, B.A., 1986. Relative Sea-level change in the Beauly Firth, Scotland. Boreas 15 (2), 191–207.
- Hammer, Ø., Harper, D.A.T., Ryan, P.D., 2001. PAST: Paleontological statistics software package for education and data analysis. Palaeontol. Electron. 4 (1), 9. http://palaeo-electronica.org/2001_1/past/issuel_01.htm.
- Hassan, G.S., Espinosa, M.A., Isla, F.I., 2009. Diatom-based inference model for paleosalinity reconstructions in estuaries along the northeastern coast of Argentina: Palaeogeography, Palaeoclimatology. Palaeoecology 275 (1–4), 77–91.
- Hawkes, A.D., Horton, B., Nelson, A., Hill, D., 2010. The application of intertidal foraminifera to reconstruct coastal subsidence during the giant Cascadia earthquake of AD 1700 in Oregon, USA. Quat. Int. 221, 116–140.
- Hemphill-Haley, E., 1995a. Diatom evidence for earthquake-induced subsidence and tsunami 300 years ago in southern coastal Washing. Geol. Soc. Am. Bull. 107, 367–378.
- Hemphill-Haley, E., 1995b. Intertidal diatoms from Willapa Bay, Washington: applications to studies of small-scale sea-level changes. Northwest Sci. 69, 29–45.
- Hemphill-Haley, E., 1996. Diatoms as an aid in identifying late-Holocene tsunami deposits. The Holocene 6 (4), 439–448.
- Hendy, N., 1964. An introductory account of the smaller algae of British Coastal Waters. In: V: Bacillariophyceae (Diatoms), pp. 1–317.
- Hirst, H., Chaud, F., Delabie, C., Jütner, I., Ormerod, S.J., 2004. Assessing the short-term response of stream diatoms to acidity using inter-basin transplantations and chemical diffusing substrates. Freshw. Biol. 49, 1072–1088.
- Hocking, E.P., Garrett, E., Cisternas, M., 2017. Modern diatom assemblages from Chilean tidal marshes and their application for quantifying deformation during past great earthquakes. J. Ouat. Sci. 32 (3), 396–415.
- Horton, B.P., Edwards, R.J., 2005. The application of local and regional transfer functions to the reconstruction of Holocene Sea levels, North Norfolk, England, 2005. Holocene 15, 216–228.
- Horton, B., Edwards, R., Lloyd, J., 1999. A foraminiferal-based transfer function: implications for sea-level studies. J. Foramin. Res. 29 (2), 117–129.
- Horton, B.P., Corbett, R., Culver, S.J., Edwards, R.J., Hillier, C., 2006. Modern saltmarsh diatom distributions of the Outer Banks, North Carolina, and the development of a transfer function for high resolution reconstructions of sea level. Estuar. Coast. Shelf Sci. 69 (3-4), 381–394.
- Horton, B.P., Zong, Y., Hillier, C., Engelhart, S., 2007. Diatoms from Indonesian mangroves and their suitability as sea-level indicators for tropical environments. Mar. Micropaleontol. 63 (3–4), 155–168.
- Horton, B.P., Milker, Y., Dura, T., Wang, K., Bridgeland, W.T., Brophy, L.S., Ewald, M., Khan, N., Engelhart, S.E., Nelson, A.R., Witter, R.C., 2017. Microfossil measures of rapid sea-level rise: timing of response of two microfossil groups to a sudden tidal-flooding experiment in Cascadia. Geology 45 (6), 535–538.
- Hustedt, F., 1937. Systematische und okologische Untersuchungen der Diatomeen floren von Java, Bali, Sumatra. Arch. Hydrobiol. Suppl. 15, 131–506.
- Hustedt, F., 1939. Systematische und okologische Untersuchungen der Diatomeen floren von Java, Bali, Sumatra. Arch. Hydrobiol. Suppl. 16, 1–394.
- Hustedt, F., 1953. Diatomeen ausdem Naturschutzpark Seeon. Archiv für. Hydrobiologie 47, 625–635.
- Hustedt, F., 1957. Die Diatomeenflora des Fluss-systems der Weser im Gebiet der Hansestadt Bremen. Abhandlungen vom Naturwissenschaftlichen Verein zu Bremen 4, 181–440.
- Hutchins, D.A., Bruland, K.W., 1998. Iron-limited diatom growth and Si: N uptake ratios in a coastal upwelling regime. Nature 393 (6685), 561.
- Jones, V., Juggins, S., 1995. The construction of a diatom-based chlorophyll a transfer function and its application at three lakes on Signy Island (maritime Antarctic) subject to differing degrees of nutrient enrichment. Freshw. Biol. 34 (3), 433–445.
- Juggins, S., 2012. C2 A program for analysing and visualising palaeoenvironmental data Version 1.7.7. University of Newcastle, Newcastle upon Tyne, UK (http://www.staff. ncl.ac.uk/stephen.juggins).
- Kemp, A.C., Cahill, N., Engelhart, S.E., Hawkes, A.D., Wang, K., 2018. Revising Estimates of Spatially Variable Subsidence during the A.D. 1700 Cascadia Earthquake using a Bayesian Foraminiferal Transfer Function.
- Kosugi, M., 1987. Limiting factors on the distribution of benthic diatoms in coastal regions salinity and substratum. Diatom 3, 21–31.
- Krammer, K., Lange-Bertalot, H., 1986. Bacillarophyceae 2/1. Naviculaceae. In: Ettl, H., Gerloff, J., Heynig, H., Mollenhauser (Eds.), Süsswasserflora von Mitteleuropa. Gustav Fischer Verlag, Stuttgart.
- Krammer, K., Lange-Bertalot, H., 1988. Bacillarophyceae 2/2. Basillariaceae, Epithemiaceae, Surirellaceae. In: Ettl, H., Gerloff, J., Heynig, H., Mollenhauser (Eds.), Süsswasserflora von Mitteleuropa. Gustav Fischer Verlag, Stuttgart.
- Krammer, K., Lange-Bertalot, H., 1991a. Bacillarophyceae 2/3. Centrales, Fragilariaceae, Eunotiaceae. In: Ettl, H., Gerloff, J., Heynig, H., Mollenhauser (Eds.), Süsswasserflora von Mitteleuropa. Gustav Fischer Verlag, Stuttgart.
- Krammer, K., Lange-Bertalot, H., 1991b. Bacillarophyceae 2/4. Achnanthaceae, Kritische Erganzungen zu Navicula (Lineolatae) und Gomphonema. In: Ettl, H. (Ed.), Pascher's Süsswasserflora von Mitteleuropa 2(4). Gustav Fischer Verlag, Stuttgart.

- Lange, K., Liess, A., Piggott, J.J., Townsend, C.R., Matthaei, C.D., 2011. Light, nutrients and grazing interact to determine stream diatom community composition and functional group structure. Freshw. Biol. 56 (2), 264–278.
- Lepš, J., Šmilauer, P., 2003. Multivariate Analysis of Ecological Data using CANOCO. Cambridge University Press, Cambridge.
- MacArthur, R.H., 1957. On the relative abundance of bird species. In: Proceedings of the National Academy of Science, USA, 43, pp. 257–288.
- Maechler, M., Rousseeuw, P., Struyf, A., Hubert, M., Hornik, K., 2019. clsuter: Cluster Analysis Basics and Extensions. R package version 2.1.0.
- McIntire, C.D., 1978. The distribution of estuarine diatoms along environmental gradients: a canonical correlation. Estuar. Coast. Mar. Sci. 6 (5), 447–457.
- Milker, Y., Nelson, A.R., Horton, B.P., Engelhart, S.E., Bradley, L.-A., Witter, R.C., 2016. Differences in coastal subsidence in southern Oregon (USA) during at least six prehistoric megathrust earthquakes. Quat. Sci. Rev. 142, 143–163.
- National Climatic Data Center, and Ncdc, 2019. "COOP Select State." IPS Record of Climatological Observations Select State | IPS | National Climatic Data Center (NCDC). NOAA. www.ncdc.noaa.gov/IPS/coop/coop.html.
- National Centers for Environmental Information, 2016. NOAA NOS Estuarine Bathymetry - Willapa Bay (P270). National Centers for Environmental Information, NOAA. doi:10.7289/V5HD7T0G [access date: May 01, 2016].
- Nelson, A.R., Kashima, K., 1993. Diatom zonation in southern Oregon tidal marshes relative to vascular plants, foraminifera, and sea level. J. Coast. Res. 673–697.
- Nelson, A.R., Sawai, Y., Jennings, A.E., Bradley, L.-A., Gerson, L., Sherrod, B.L., Sabean, J., Horton, B.P., 2008. Great-earthquake paleogeodesy and tsunamis of the past 2000 years at Alsea Bay, Central Oregon coast, USA. Quat. Sci. Rev. 27 (7–8), 747, 769
- Nelson, A.R., Hawkes, A.D., Sawai, Y., Horton, B.P., Witter, R.C., Bradley, L.-A., Cahill, N., 2020. Minima stratigraphic evidence for coseismic coastal subsidence during 2000 yr of megathrust earthquakes at the central Cascadia subduction zone. Geosphere 16. https://doi.org/10.1130/GES02254.1.
- NOAA, 2019. "NOAA Tides & Currents." Station Home Page NOAA Tides & Currents. ti desandcurrents.noaa.gov/stationhome.html?id=9440846.
- O'Donnell III, R.J., 2017. Geochemical Variance Of Salt Marshes along the Cascadian Subduction Zone and their Utility in Estimating Coseismic Subsidence (Masters Thesis). University of North Carolina, Wilmington.
- Oemke, M.P., Burton, T.M., 1986. Diatom colonization dynamics in a lotic system. Hydrobiologia 139 (2), 153–166.
- Olabarrieta, M., Warner, J.C., Kumar, N., 2011. Wave-current interaction in Willapa Bay. Journal of Geophysical Research 116, C12014. https://doi.org/10.1029/ 2011JC007387.
- Padgett, J.S., Engelhart, S.E., Kelsey, H.M., Witter, R.C., Cahill, N., Hemphill-Haley, E., 2021. Timing and Amount of Southern Cascadia Earthquake Subsidence over the Past 1700 Years at Northern Humboldt Bay. California, USA.
- Palmer, A.J., Abbott, W.H., 1986. Diatoms as Indicators of Sea-Level Change. Springer, Sea-level Research, pp. 457–487.
- Peletier, H., 1996. Long-term changes in intertidal estuarine diatom assemblages related to reduced input of organic waste. Mar. Ecol. Prog. Ser. 137, 265–271.
- R Core Development Team, 2020. R: A Language and Environment for Statistical Computing. R Foundation for Statistical Computing, Vienna. https://www.R-project. org/.
- Sabean, J.A., 2004. Applications of Foraminifera to Detecting Land Level Change
 Associated with Great Earthquakes along the West Coast of North America. Theses
 (Dept. of Earth Sciences)/Simon Fraser University.
- Sarthou, G., Timmermans, K.R., Blain, S., Tréguer, P., 2005. Growth physiology and fate of diatoms in the ocean: a review. J. Sea Res. 53 (1–2), 25–42.
- Sawai, Y., Horton, B., Nagumo, T., 2004a. The development of a diatom-based transfer function along the Pacific coast of eastern Hokkaido, northern Japan?an aid in paleoseismic studies of the Kuril subduction zone. Quat. Sci. Rev. 23 (23–24), 2467–2483
- Sawai, Y., Satake, K., Kamataki, T., Nasu, H., Shishikura, M., Atwater, B.F., Horton, B.P., Kelsey, H.M., Nagumo, T., Yamaguchi, M., 2004b. Transient uplift after a 17thcentury earthquake along the Kuril subduction zone. Science 306 (5703), 1918–1920.
- Sawai, Y., 2001. Distribution of living and dead diatoms in tidal wetlands of northern Japan: relations to taphonomy. Palaeogr. Palaeoclimatol. Palaeocco. 173, 125–141.

- Sawai, Y., Horton, B.P., Kemp, A.C., Hawkes, A.D., Nagumo, T., Nelson, A.R., 2016. Relationships between diatoms and tidal environments in Oregon and Washington, USA. Diatom Res. 31 (1), 17–38.
- Shennan, I., Hamilton, S., 2006. Coseismic and pre-seismic subsidence associated with great earthquakes in Alaska. Quat. Sci. Rev. 25 (1–2), 1–8.
- Shennan, I., Innes, J.B., Long, A.J., Zong, Y., 1994. Late Devensian and Holocene relative sealevel changes at Loch nan Eala, near Arisaig, northwest Scotland. J. Quat. Sci. 9 (3), 261–283.
- Shennan, I., Long, A.J., Rutherford, M.M., Green, F.M., Innes, J.B., Lloyd, J.M., Zong, Y., Walker, K.J., 1996. Tidal marsh stratigraphy, sea-level change and large earthquakes: a 5000 year record in Washington, U.S.A. Quat. Sci. Rev. 15 (10), 1023–1059
- Sherrod, B., 1999. Gradient analysis of diatom assemblages in a Puget Sound salt marsh: can such assemblages be used for quantitative paleoecological reconstructions? Palaeogeogr. Palaeoclimatol. Palaeoecol. 149 (1-4), 213–226.
- Sladecek, V., 1986. Diatoms as indicators of organic pollution. Acta Hydrochim. Hydrobiol. 14 (5), 555–566.
- Smith, D.G., Meyers, R.A., Jol, H.M., 1999. Sedimentology of an upper-mesotidal (3.7 m) Holocene barrier, Willapa Bay, SW Washington, U.S.A. J. Sediment. Res. 69, 1290–1296
- Sperazza, M., Moore, J.N., Hendrix, M.S., 2004. High-resolution particle size analysis of naturally occurring very fine-grained sediment through laser diffractometry. J. Sediment. Res. 74 (5), 736–743.
- ter Braak, C.J., 1985. Correspondence analysis of incidence and abundance data: properties in terms of a unimodal response model. Biometrics 41, 859–873.
- ter Braak, C.J., 1986. Canonical correspondence analysis: a new eigenvector technique for multivariate direct gradient analysis. Ecology 67 (5), 1167–1179.
- ter Braak, C.J., Barendregt, 1986. Weighted averaging of species indicator values: its efficiency in environmental CALIBRATION. Math. Biosci. 78, 57–72.
- ter Braak, C.J., Smilauer, P., 1998. CANOCO Reference Manual and user's Guide to Canoco for Windows: Software for Canonical Community Ordination (version 5.0).
- ter Braak, C.J., Smilauer, P., 2002. CANOCO Reference Manual and CanoDraw for Windows User's Guide: Software for Canonical Community Ordination (version 4.5). www.canoco.com.
- Theriot, E., 1992. Clusters, species concepts, and morphological evolution of diatoms. Syst. Biol. 41 (2), 141–157.
- Tornés, E., Cambra, J., Gomà, J., Leira, M., Ortiz, R., Sabater, S., 2007. Indicator taxa of benthic diatom communities: a case study in Mediterranean streams. Int. J. Limnol. 43. 1–11.
- van Togeren, O.F.R., 1987. Cluster analysis. In: Jongman, R.H.G., ter Braak, C.J.F., van Tongeren, O.F.R. (Eds.), Data Analysis in Community and Landscape Ecology, pp. 174–212 (AC Wageningen).
- Vos, P.C., de Wolf, H., 1993. Diatoms as a tool for reconstructing sedimentary environments in coastal wetlands; methodological aspects. Hydrobiologia 269 (1), 285–296.
- Watcham, E.P., Shennan, I., Barlow, N.L., 2013. Scale considerations in using diatoms as indicators of sea-level change; lessons from Alaska. J. Ouat. Sci. 28 (2), 165–179.
- Witkowski, A., 2000. Diatom flora of marine coasts. In: Lange-Bertalot, H. (Ed.), Iconagraphia Diatomologica, v.7. A.R.G. Gantner, Germany.
- Woodroffe, S.A., Long, A.J., 2010. Reconstructing recent relative sea-level changes in West Greenland: local diatom-based transfer functions are superior to regional models. Ouat. Int. 221 (1–2), 91–103.
- Yang, S.L., Li, H., Ysebaert, T., Bouma, T.J., Zhang, W.X., Wang, Y.Y., Li, P., Li, M., Ding, P.X., 2008. Spatial and temporal variations in sediment grain size in tidal wetlands, Yangtze Delta: on the role of physical biotic controls. Estuar. Coast. Shelf Sci. 77. 657–671.
- Zong, Y., 1997a. Mid- and late-Holocene Sea-level changes in Roudsea Marsh, northwest England: a diatom biostratigraphical investigation. The Holocene 3 (3), 311–323.
- Zong, Y., Horton, B.P., 1998. Diatom zones across intertidal flats and coastal saltmarshes in Britain. Diatom Res. 13 (2), 375–394.
- Zong, Y., Horton, B.P., 1999. Diatom-based tidal-level transfer functions as an aid in reconstructing Quaternary history of sea-level movements in the UK. J. Quat. Sci. 14 (2), 153–167.
- Zong, Y., Shennan, I., Combellick, R., Hamilton, S., Rutherford, M., 2003. Microfossil evidence for land movements associated with the AD 1964 Alaska earthquake. The Holocene 13 (1), 7–20.